6-26-2020

Synthesizing modified polymeric nanoparticles for biofilm inhibition, antibiotic encapsulation, and specific targeting against Pseudomonas aeruginosa

Logan Schnorbus
Rowan University

SYNTHESIZING MODIFIED POLYMERIC NANOPARTICLES FOR BIOFILM INHIBITION, ANTIBIOTIC ENCAPSULATION, AND SPECIFIC TARGETING AGAINST *PSEUDOMONAS AERUGINOSA*

by

Logan Schnorbus

A Thesis

Submitted to the
Department of Chemistry and Biochemistry
College of Science and Mathematics
In partial fulfillment of the requirement
For the degree of
Master of Science in Pharmaceutical Sciences
at
Rowan University
May 7, 2020

Thesis Chair: Lark Perez, Ph.D.

Dedications

I would like to dedicate this manuscript to Susan Schnorbus. Susan has not just been a grandmother to me, but an inspiring individual, full of wisdom and motivation, that has guided me throughout my college career. Her support has helped me achieve my goals in life. I am certain she will remain an inspiring and supportive figure for years to come.

Acknowledgments

I would like to acknowledge Lark J. Perez, PhD for is compassionate and unequivocal support, not just as a mentor, but as friend and colleague. Lark, an inspiring intellectual, immensely learned and well-read, guided and trusted me throughout my journey to become a successful scientist. His outspoken advice, has helped me understand and become an increasingly motivated, passionate, and scientific individual. I am confident Lark will continue to change the world with his compassion and motivation to others and the sciences he conducts.

Moreover, I would like to thank the Rowan University chemistry & biochemistry department for the organization of the proud and home-like atmosphere is has created for its students and staff. I was fortunate to interact with key individuals, like Rich Norton, who work diligently and passionately to support this atmosphere at Rowan University. I am certain this welcoming community will continue to function as a highly successful hub for future scientists and inspiring individuals.

Abstract

Logan Schnorbus
SYNTHESIZING MODIFIED POLYMERIC NANOPARTICLES FOR BIOFILM
INHIBITION, ANTIBIOTIC ENCAPSULATION, AND SPECIFIC TARGETING
AGAINST PSEUDOMONAS AERUGINOSA
2019-2020
Lark Perez Ph.D.
Master of Science in Pharmaceutical Sciences

Widespread usage of antibiotics is a growing concern due to antibiotic resistance development in bacteria. This is due to common use of antibiotics in agricultural, livestock, and clinical usage. New strategies in drug development are necessary to combat the increasing resistance. We designed several motifs of sugar-modified nanoparticles to inhibit the biofilm formation of *Pseudomonas aeruginosa*.

P. aeruginosa is an opportunistic pathogenic bacterium that is responsible for common life-threatening infection in hospitals. This gram-negative opportunistic pathogenic bacterium infects hosts with compromised immune systems and contributes to complications in patients suffering from pneumonia, cystic fibrosis, and other immune compromising conditions. Biofilm formation from *P. aeruginosa* is used as an attack mechanism and adds to antibiotic resistance.

P. aeruginosa lectins, LecA and LecB, are two sugar-binding proteins distinct in structure, binding preference and involvement of biofilm formation in this pathogen. Lectins, LecA and LecB, are specific to D-galactose, and L-fucose, respectively. Modifying the surface of our nanoparticle with the lectin-specific sugars achieves lectin binding selectivity, biofilm inhibition, and the ability to introduce antibiotic encapsulation, which could lead to pathogen-specific use of antibiotics.

Table of Contents

Table of Contents (Continued)

Table of Contents (Continued)

List of Figures

List of Figures (Continued)

List of Tables

List of Schemes

Chapter 1

Inhibition of *Pseudomonas aeruginosa* Biofilm Formation with Surfaced Modified Polymeric Nanoparticles

1. Introduction

The ongoing increase of antibiotic resistance represents a significant challenge to modern medicine [1–3]. Due to the widespread use of antibiotics in clinical and agricultural settings and the limited number of novel antibiotics being advanced into the market, the development of new treatment options for bacterial infection is of paramount importance.

Pseudomonas aeruginosa represents one of the most significant gram-negative opportunistic pathogens involved in hospital-acquired infections. A report from the CDC-NNIS (National Nosocomial Infections Surveillance, US Dept. of Health and Human Services) identifies *P. aeruginosa* as the second leading cause of pneumonia, the third leading cause of urinary tract infection, and the eighth most frequently isolated pathogen from the bloodstream [1–7]. Further, *P. aeruginosa* often causes lethal infections in cystic fibrosis and immunocompromised patients, for whom the formation of bacterial biofilms plays a central role in infection and resistance [8,9]. Given the rapidly increasing incidence of *P. aeruginosa* in the clinic coupled with the high levels of antibiotic resistance and production of copious biofilms often found with this pathogen, the development of novel treatment strategies is imperative [10–12].

In *P. aeruginosa*, biofilm formation is regulated by a cell-cell communication mechanism known as quorum sensing, which is mediated by bacterial cell-surface lectins involved in cellular adhesion [13,14]. Specifically, the galactose-binding lectin LecA (PA-

IL) and the fucose-binding lectin LecB (PA-IIL) have prominent roles in bacterial virulence, cellular adhesion, tissue colonization, and/or invasion and biofilm formation [15–17]. Several recent reports have evaluated approaches to inhibit the virulence and/or biofilm formation in *P. aeruginosa* through inhibition of quorum sensing or lectin binding. Notable about these anti-virulence approaches is the potential they possess for species-selectivity by targeting the inhibition of cellular processes in a manner that uniquely inhibits the virulence and/or infectivity of *P. aeruginosa*. Accordingly, treatments developed for these *P. aeruginosa*-specific targets are anticipated to have a lower impact on the beneficial commensal bacterial population and may possibly exhibit reduced pressure for the development of antibiotic resistance.

Prior studies developing inhibitors of *P. aeruginosa* LecA have described mono-valent and multi-valent inhibitors of this lectin and have characterized the positive effect on inhibitor avidity through multivalency [12,17]. We rationalized that we might achieve similar high binding avidity for LecA using a polymeric nanoparticle with multiple copies of a LecA ligand on the surface of the particle. Further, we recognized that unlike dendrimeric or small molecule inhibitors of LecA, the surface-modified polymeric nanoparticles that we aimed to prepare would be capable of encapsulating a fluorescent or drug molecule within their lipophilic core, potentially enabling future applications in targeted antibiotic drug delivery or fluorescent labeling for diagnostic applications. Here we report our findings on the development and anti-biofilm properties of a series of LecA-targeted polymeric nanoparticles.

2. Results

2.1 Synthesis of galactose-modified di-block do-polymer. The D-galactose-modified di-block co-polymer required for nanoparticle assembly (**5**) was prepared from β-D-galactose pentaacetate in six steps (Scheme 1). In short, β-D-galactose pentaacetate (**1**) was coupled to benzyl 4-hydroxybenzoate (**2**) to provide ester **3**. Removal of the benzyl protecting group by hydrogenolysis provided carboxylic acid **4**, which was coupled to 6.6 kD amine terminated di-block co-polymer [18]. Removal of the acetate protecting groups on the sugar preceded purification of the sugar-modified polymer **1** by dialysis using a 5 kD molecular weight cutoff (MWCO) membrane. The resulting dialyzed D-galactose-modified polymer (**5**) was concentrated by lyophilization and the resulting white powder was characterized by NMR, IR, and MALDI-MS. Having prepared the requisite galactose-modified di-block copolymer **5**, we proceeded with the assembly of polymeric nanoparticles.
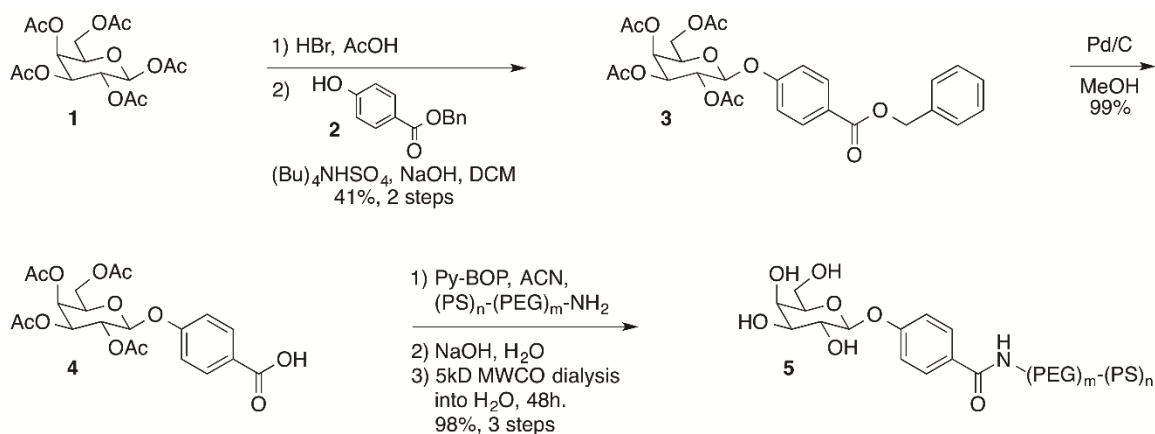
Scheme 1. Synthesis of modified di-block co-polymer for nanoparticle assembly. Abbreviations: DCM, dichloromethane; CAN, acetonitrile; MWCO, molecular weight cutoff

2.2 Nanoparticle preparation. Nanoparticles were prepared by flash nanoprecipitation using established methods [18,19] with varying ratios of the modified D-galactose polymer and unmodified di-block co-polymer to provide 100%-, 50%-, and 25%-surface-modified nanoparticles using the parameters described in Table 1. All nanoparticles were prepared using racemic α-tocopherol (vitamin E) as an inert core stabilizer.

Table 1

Summary of polymeric nanoparticle (NP) prepared with varying levels of surface modification

Formulation	Active Stabilizer		Stabilizer		Inert Core		NP Properties	
	Block co-polymer	Conc. (mg/mL)	Block co-polymer	Conc. (mg/mL)	Filler	Conc. (mg/mL)	Z-diameter (nm)[1]	PDI[2]
0%	PS-*b*-PEG-Gal	0.00	PS-*b*-PEG	0.40	Vit E	0.40	88.83±4.64	0.0327
25% Gal-NP	PS-*b*-PEG-Gal	0.10	PS-*b*-PEG	0.30	Vit E	0.40	73.78±2.23	0.0132
50% Gal-NP	PS-*b*-PEG-Gal	0.20	PS-*b*-PEG	0.20	Vit E	0.40	74.74±2.26	0.0083
100% Gal-NP	PS-*b*-PEG-Gal	0.40	PS-*b*-PEG	0.00	Vit E	0.40	81.47±12.75	0.2693

Data represent the mean with error described as the standard error of means of at least three independent preparations of the particles, each with three instrumental replicates. [2] Polydispersity Index (PDI) = (standard deviation/mean diameter) $^{\wedge 2}$. Abbreviations: VitE, vitamin E (α-tocopherol).

All D-galactose nanoparticle (Gal-NP) suspensions were prepared as 0.02 mg/mL solutions in water and characterized in terms of particle diameters (Figure 1) and polydispersity indexes (PDI). The particles prepared are described in this manuscript based

on the relative concentration of surface-modified D-galactose to enable direct comparison of the effect of the prepared nanoparticles on lectin binding and biofilm inhibition to free D-galactose, used as a control. Having prepared a series of galactose-modified polymeric nanoparticles, we conducted an evaluation of the lectin binding properties of the prepared particles.
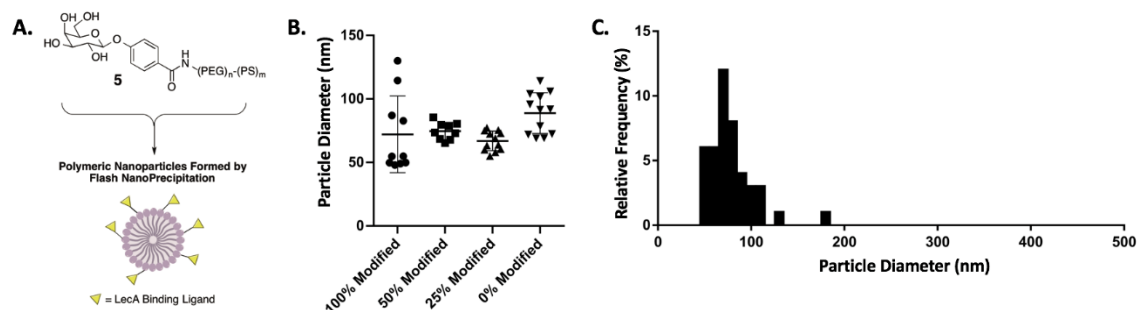
Figure 1. Schematic showing assembly of D-galactose surface-modified polymeric nanoparticles. B. Particle size distribution of prepared polymeric nanoparticles. Each data point represents the average particle diameter of an independent formulation. C. Histogram of particle size distribution for all nanoparticles prepared in this study.

2.3 Inhibition of LecA-mediated hemagglutination. The binding affinity of the modified nanoparticles for the *P. aeruginosa* lectin LecA was evaluated using a hemagglutination assay [20]. Briefly, this assay measures the inhibition of LecA-induced hemagglutination of rabbit erythrocytes by comparison with D-galactose as a control. The exceptional effect of ligand multivalency was noted with the 100%- and 50%-modified NP samples, which were evaluated based on the concentration of galactose on the surface of the nanoparticles (Table 2). The strongest effect was observed with the 50%-modified Gal-NP, showing a 992-fold increase in relative potency compared with free galactose. The

100%-modified Gal-NP samples inhibited hemagglutination when modified with concentrations above 6.31µM of galactose, representing a 495-fold increase in potency relative to free galactose. The 25%-modified NP showed no inhibition of hemagglutination up to the highest surface concentration of D-galactose evaluated (2.36 µM). A control 100%-mannose-modified polymeric NP (37.9 µM mannose) showed no inhibition of hemagglutination, supporting the hypothesis that the inhibition of LecA is mediated by specific interactions between the lectin and the nanoparticle surface only with galactose modification.

Table 2

Inhibition of P. aeruginosa LecA-induced hemagglutination.

Entry	Formulation	Hemagglutination Assay MIC (uM)[1]	Relative Potency[4]
1	D-galactose	3125.0	1.0
2	100%-Modified D-galactose-NP	6.31	495.2
3	50%-Modified D-galactose-NP	3.15	992.1
4	25%-Modified D-galactose-NP	none[2]	-
5	100%-Modified mannose-NP	none[3]	-

MIC = minimal inhibitory concentration for the hemagglutination assay following two-fold serial dilutions of tested compounds; the MIC corresponds to the highest dilution resulting in the inhibition of LecA-induced hemagglutination based on the relative sugar concentration. [2] No inhibition of hemagglutination up to highest concentration evaluated (galactose concentration of 2.36μM). [3] No inhibition of hemagglutination up to highest concentration evaluated (maltose concentration of 37.9μM). [4] Relative potency based on concentration of galactose = ($MIC_{(D\text{-}galactose)}/MIC_{(ligand)}$).

The high potency of the particles in this assay is consistent with previous reports of high avidity LecA binding using galactose modified dendrimers [12,20]. It is noted that the % modification of the particle leads to maximal inhibition with the 50%-sugar-modified particles. Particles with lower galactose modification (25%-modified) showed no inhibition of hemagglutination at the highest concentrations tested ([galactose] = 2.36 μM) and those with higher modification (100%-modified) had a two-fold higher MIC. It is possible that a sugar concentration greater than 2.36 μM on the nanoparticles is required for high avidity; however, higher sugar concentrations as would be present in the 100%-modified nanoparticles result in the steric inhibition of lectin binding.

2.4 Inhibition of P. aeruginosa PAO1 biofilm formation. Having identified that our 100%- and 50%-D-galactose-modified polymeric nanoparticles are effective at inhibiting LecA-induced hemagglutination, we evaluated their effect on bacterial biofilm formation using the well-established crystal violet assay [21,22]. Briefly, *P. aeruginosa* strain PAO1 was inoculated in 96-well plates in the presence of varying concentrations of Gal-NP, controls, and/or free D-galactose. Biofilm formation was evaluated after 24 h by removing non-adherent bacteria, crystal violet staining of the adherent cells, and determination of absorbance at 550nm. In this assay, we observed a potent dose-dependent inhibition of biofilm formation with our surface-modified Gal-NP samples (Figure 2). Inhibition of biofilm formation was noted at D-galactose concentrations above 12.6 μM in the 100%-surface-modified nanoparticle samples and at concentrations above 6.3 μM in the 50%-surface-modified series. Again, the significance of ligand valency is evident, as free D-galactose, even at 32,000 μM, showed no inhibition of biofilm formation in this assay.
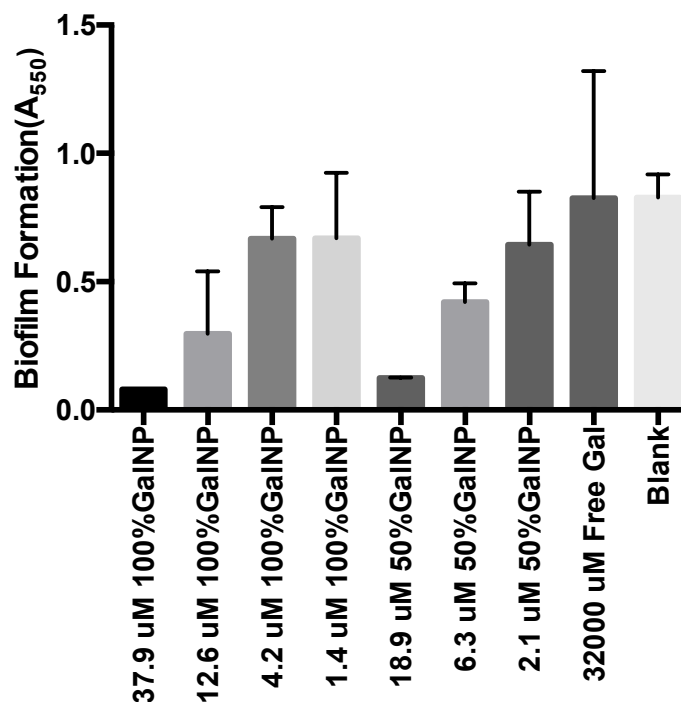
Figure 2. Inhibition of *P. aeruginosa* PAO1 biofilm formation based on the crystal violet assay. Surface-modified Gal-NP samples are described based on the % surface modification and the relative concentration of D-galactose on the nanoparticle surface. All data points are described as the mean of triplicate measurements with error bars representing the standard deviation.

2.5 Evaluation of growth inhibition. No significant inhibition of growth was noted at any of the nanoparticle concentrations evaluated in our biofilm inhibition assay. The absence of growth inhibition supports the hypothesis that that nanoparticle-LecA binding interactions inhibit bacterial biofilm formation via an antivirulence (non-antibiotic) mechanism.
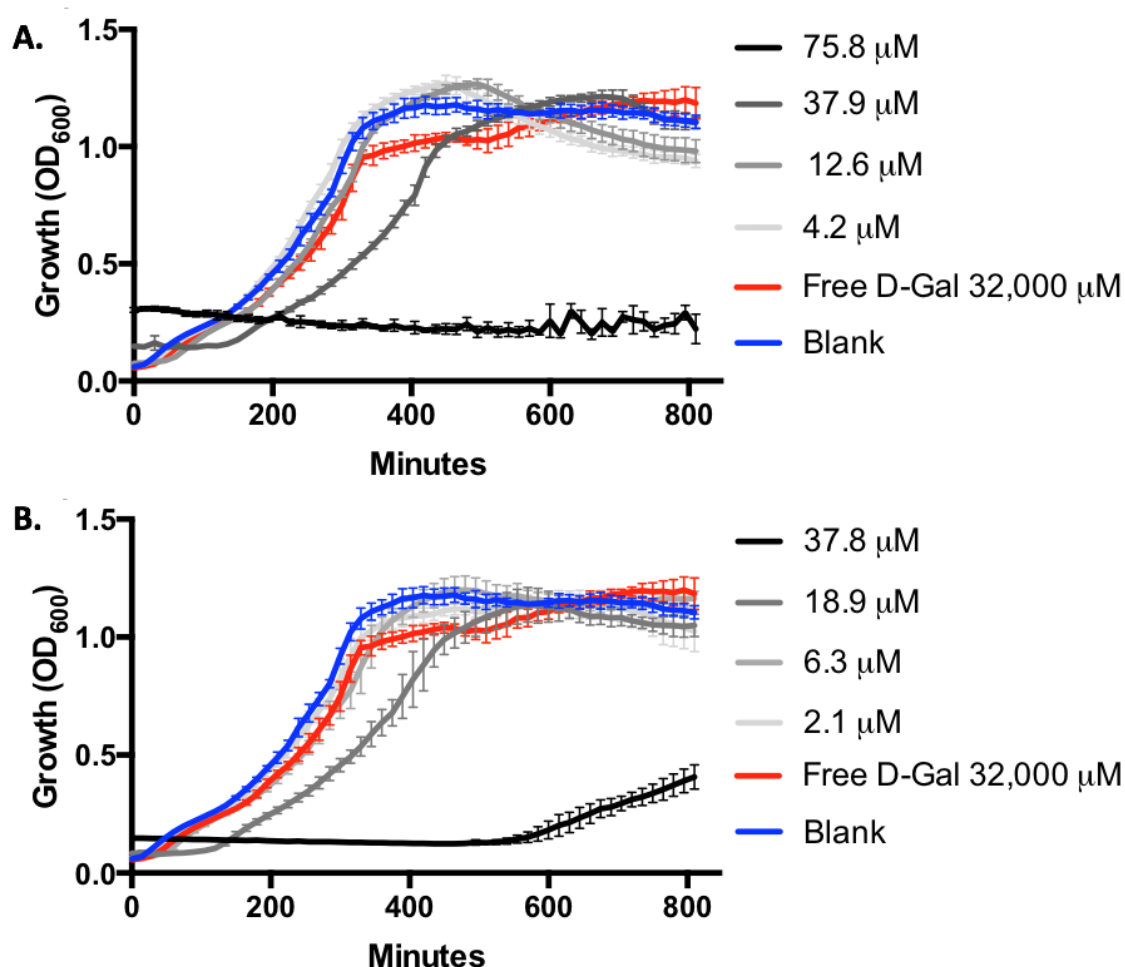
Figure 3. Evaluation of *P. aeruginosa* PAO1 growth by monitoring OD_{600} with 100%-D-galactose-surface-modified nanoparticles (A) and 50%-D-galactose-surface-modified nanoparticles (B). No significant growth inhibition is observed with 100%-modified Gal-NP at concentrations below 37.9 μM or with 50%-modified Gal-NP at concentrations below 18.9 μM. Growth inhibition was noted at concentrations two-fold higher than those employed in the biofilm inhibition assays (100% Gal-NP at 75.8 μM and 50% Gal-NP at 37.8 μM). Error bars represent standard deviation of triplicate analysis.

2.6 Evaluation of biofilm inhibition and morphology. We subsequently evaluated the inhibition of biofilm formation in the hyper-virulent isolate of *P. aeruginosa* PA14 by fluorescent confocal microscopy. Briefly, 24-h biofilms were prepared by inoculation of PA14-GFP [23] into Luria broth (LB) containing the appropriate treatments or controls.

10

The resulting biofilm was then evaluated by fluorescent confocal microscopy. In this experiment, we observed clear changes in the overall biomass and average biofilm thickness of the Gal-NP-treated samples, consistent with our observations in the crystal violet assay. Additionally, in this experiment, we captured distinct changes in the morphology of the biofilm that are evident at sub-inhibitory concentrations. These observations further support the inhibition of cellular adhesion by D-galactose surface modified nanoparticles.

Within the 100%- and 50%-surface-modified samples of nanoparticles we observed the inhibition of biofilm formation based on evaluation of biofilm biomass and average biofilm thickness at concentrations above ~19.5 μM; however, effects on biofilm morphology were apparent at even lower concentrations (Figure 4). The slightly higher concentrations required to inhibit biofilm formation in the hypervirulent PA14 strain, compared with our crystal violet assay with PAO1, are consistent with previous studies of this bacteria [24,25]. In this assay, we observed no inhibition of biofilm formation by free D-galactose, even at concentrations of 48,000 μM (Figures 4 and 5). Visual inspection of the images collected (Figure 4 and Supporting Information) show that with increasing concentration of D-galactose-modified nanoparticles the biofilm begins to display increasing numbers of spaces within the biofilm structure (Figure 4, panel A vs. B vs. D). This effect is consistent with the anticipated inhibition of cellular adhesion achieved by inhibiting the activity of LecA in the presence of Gal-modified nanoparticles.

| 100% modified NP [Gal]=38μM | 100% modified NP [Gal]=9.75μM | Free Galactose [Gal]=48000μM | Blank |
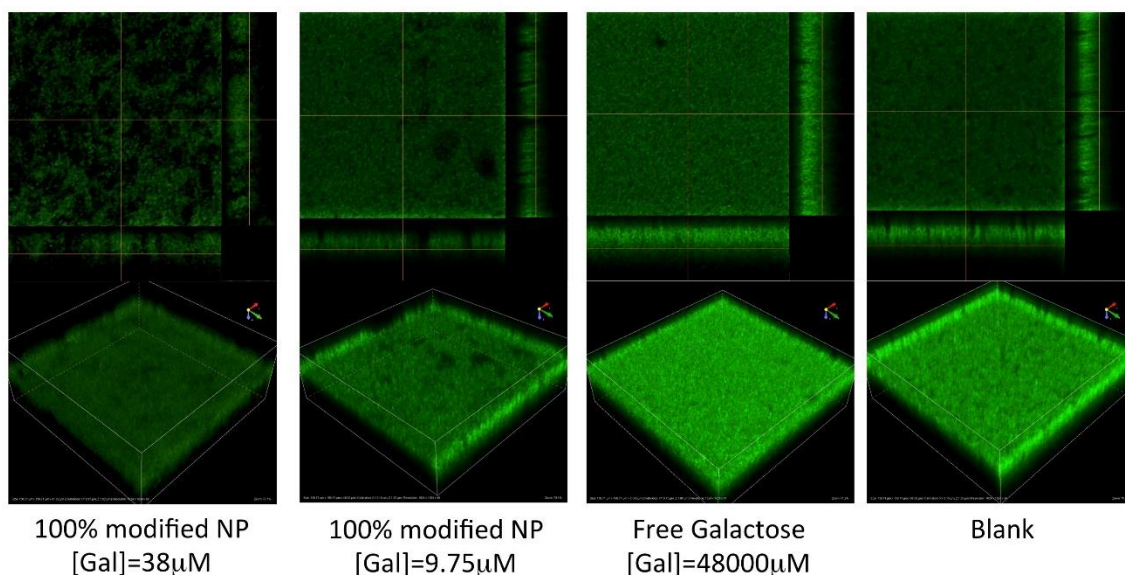
Figure 4. Fluorescent confocal microscopy evaluation of *P. aeruginosa* PA-14 biofilms. Samples treated with Gal-NP show inhibition of biofilm formation. The biofilm morphology at sub-inhibitory concentrations of Gal-NP (e.g. 100%-modified at 9.75 μM) shows evidence of anti-adhesive properties of Gal-NP, which increase with higher concentrations. For additional images see Supporting Information.

Quantification of the biomass and average biofilm thickness of the confocal images using the program Comstat2 shows dose-dependent inhibition of biofilm formation (Figures 5A and B). Most striking is the quantification of biofilm surface area as a function of volume. This calculation nominally provides a measure of the quantity/size of spaces within the biofilm structure. Consistent with the hypothesis that Gal-NP inhibit cellular adhesion without inhibiting growth/viability, we observe a dose-dependent increase in the biofilm surface area/volume (Figure 5C).
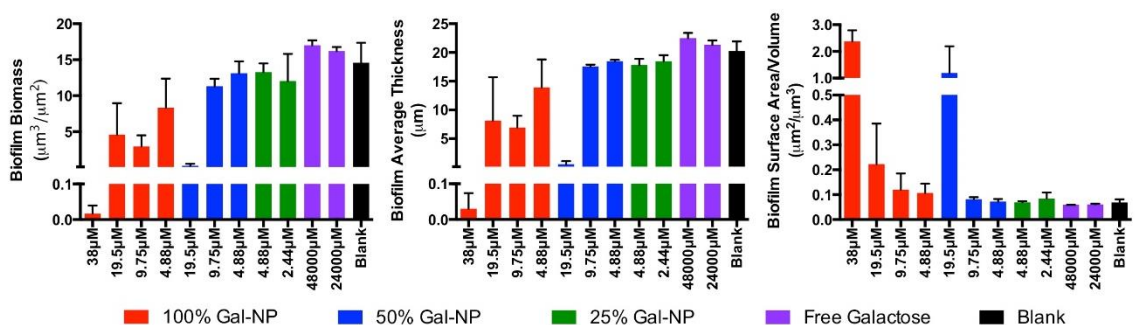
Figure 5. Quantification of (a) biofilm total biomass, (b) average biofilm thickness, and (c) biofilm surface area/volume from fluorescent confocal microscopy analysis. Images were analyzed using Comstat2 processing of duplicate analysis and are reported as means with error bars representing standard deviations.

3. Discussion

Recently, significant interest has been directed at the development of antivirulence strategies to combat infectious diseases. As these approaches do not directly impact viability or growth, a reduced selective pressure for resistance is anticipated. For the inhibition of biofilm formation, many antivirulence agents being developed focus on the inhibition of the quorum-sensing signaling pathways [14,24,26] or inhibition of bacterial adhesion [20,27,28]. Bacterial lectins are implicated in key roles in bacterial adhesion and biofilm formation, including the lectins LecA and LecB, which play a prominent role in *P. aeruginosa*. Here we report the development of the first LecA-targeted surface-modified polymeric nanoparticle. The particles prepared showed high avidity for LecA in the inhibition of hemagglutination, consistent with a beneficial effect of multivalent display of the lectin ligand on the particle surface. We observed greater than 100-fold enhancement in potency, compared with free D-galactose in the assay with 100%- and 50%-surface modified D-galactose nanoparticles. Further, we demonstrated potent inhibition of *P. aeruginosa* biofilm formation in the presence of these surface-modified nanoparticles,

13

demonstrating the anti-virulence potential of these novel inhibitors of the *P. aeruginosa* lectin LecA.

Previous studies have shown that LecA is cytotoxic [29] and has an important role in cellular adhesion and lung infection [17]. LecA is a homotetramer and displays specificity for galactose. Due to the high affinity of LecA for galactose, numerous multivalent and dendrimer structures have been developed as inhibitors of this protein [12,20,27,28]. The significant increase in LecA binding potency noted in these dendrimeric constructs was captured in the polymeric nanoparticles in this study, which were found to be potent inhibitors of LecA-induced hemagglutination and bacterial biofilm formation.

Notably, the assembly of nanoparticles as highly multivalent scaffolds for lectin binding avoids many of the synthetic challenges of dendrimer synthesis [30,31]. Accordingly, we anticipate that the application of polymeric nanoparticles to achieve the high lectin-binding potency observed with dendrimers, as demonstrated here, will serve as a powerful and useful complimentary approach for the inhibition of bacterial lectins and other cell-surface receptors. Self-assembly of sugar-modified di-block co-polymers using flash nanoprecipitation [19] further enables ready introduction of multiple different ligands to enable targeting multiple biological targets with a single nanoparticle construct, further enhancing biological activity.

Polymeric nanoparticles have been extensively studied in several medical technologies, especially in the area of drug delivery [11,32–37]. The advantages of improved pharmacokinetics and therapeutic properties, including mucus penetration [38], continue to stimulate interest in the field. As demonstrated here, surface modification of the nanoparticle enables targeting of the constructs to the bacterial pathogens of interest,

potentially enabling species-specific delivery of drugs, diagnostic reagents, or other small molecules.

4. Conclusion

In conclusion, polymeric nanoparticles synthetically modified to provide surface display of conjugated D-galactose bind to the *P. aeruginosa* lectin LecA with high potency. The benefit of high ligand valency to achieve high avidity lectin binding is efficiently realized in these constructs. Several of the polymeric nanoparticles were found to inhibit biofilm formation in a manner consistent with an antivirulence (anti-adhesion) mechanism of action, providing a new and powerful technology for species-specific inhibition of bacterial virulence.

Chapter 2

Synthesis of Multivalent Galactose Modified Polymers

5. Introduction

Our first-generation NPs, mono-modified galactose NPs, provided strong

evidence to support the ability to combat *P. aeruginosa,* and antibiotic resistance.

Observation of polymer-linked galactose nanoparticles displayed a notable effect, where

50%-modified Gal-NP showed a 992-fold increase in relative potency compared with

free galactose. Observation of no activity above 38,000 µM of free galactose could be

contrasted to the 38 µM of galactose on the surface of nanoparticles. This provided

evidence that localization due to surface modification is necessary for galactose to have

LecA activity and that free galactose alone would not be enough. Furthermore,

examination into unmodified nanoparticles and mannose surface-modified nanoparticles

provided no activity against *P. aeruginosa.*

The next step of our project, following the success of our first-generation mono-

modified galactose nanoparticles, was to shift direction towards improving our

nanoparticles by increasing the valency of galactose per unit polymer. For instance, we

hypothesized that a di-valent galactose, where two galactoses are attached per unit

polymer, would be more active than our previous mono-galactose NP modification.

Further, we anticipate that tetra-modified galactose nanoparticles, where the surface of

the nanoparticles has four times the concentration of galactose than our first-generation

mono-galactose modified nanoparticles will provide even higher activity. To test this

hypothesis, we designed, evaluated and optimized a series of synthetic schemes involving

lysine modification, cyanic chloride, and other linker materials to achieve multivalent galactose-polymers.

6. Results

6.1 Synthesis of mono-boc benzyl-diamine linker. Lysine was chosen to be a linking molecule due to its functional group identity. Two amines and a carboxylic acid are available for modification. We recognized that attaching galactose molecules to lysine's amines and using the acid on lysine for linkage to the polymer to give a di-valent galactose functionalized nanoparticle. Unfortunately, direct coupling of the modified lysine to the polymer through direct reaction of the carboxylic acid on lysine proved difficult. Optimization of synthetic route lead to addition of a diamine linker, which would provide ease in coupling of the lysine carboxylic acid to our di-block copolymer. This diamine linker, was optimized to be protected at one single amine using one Boc (tert-Butyloxycarbonyl) protection group (Scheme 2).
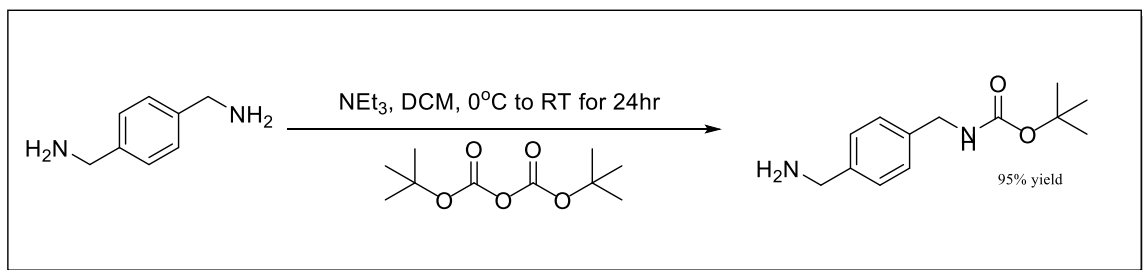
Scheme 2. Synthesis of mono-boc protected benzyl-diamine linker for galactose modified lysine.
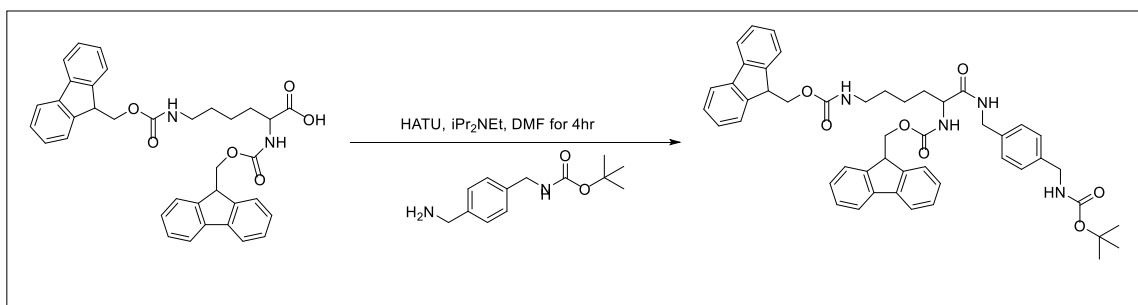
Scheme 3. Synthesis of Fmoc and Boc protected lysine-diamine-linker.

6.2 Synthesis of bis-galactose PS-PEG. Lysine-Galactose coupling was achieved after trials with a series of coupling reagents and conditions. The coupling of bis-Fmoc (Fluorenylmethyloxycarbonyl) amine protection on lysine and Boc protection for diamine linkage proved to be the most effective method to prepare lysine for sugar-polymer couplings (Scheme 3). Specifically, HATU coupling followed by direct product precipitation was found to be best for product yield (Table 3). While an isolated yield of approximately 35% is non-ideal for this reaction, it appears that the majority of the material lost in this reaction is due to the difficulty in product purification/isolation. Direct precipitation provides the highest yield for this process and as starting materials are readily accessed we elected to proceed forward with our synthesis.

Table 3

Amine coupling reagents for lysine-diamine coupling

Coupling Reagent	Reaction Time (Hours)	Product Yield (%)	Work-Up/Purification
BOP	14	< 1	standard
PyBOP	14	< 1	standard
HATU	14	< 1	standard
BOP	3	26	standard
PyBOP	4	10	standard
HATU	2	24	standard
HATU	2	35	direct product precipitation

Note. Coupling reagents used to bind galactose and lysine via diamine linker. Reaction was performed as an amide coupling with HATU at 35% yield.

Having prepared the required lysine with our polymer linker in place, we turned our attention to the removal of the Fmoc protecting groups and incorporation of our required galactose sugars on lysine. Fmoc deprotection with DBU (1,8-Diazabicyclo(5.4.0)undec-7-ene) followed by ether trituration precipitated free-amine lysine. The crude product was immediately exposed to previously galactose derivatives for PyBop assisted amide coupling (Scheme 4). Following purification, we were pleased to confirm the structure of the desired bis-galactose modified lysine through NMR analysis (Figure 6 and Supporting Information). Some key signals in the ^{1}H-NMR spectra (Figure 6), include the presence of 4 distinct methyl singlets at ~2 ppm which correspond to the four distinct acetate groups on the coupled galactose fragments and the methyl singlet at ~1.2 ppm which corresponds to the Boc-protecting group on the linker attached to lysine. Additionally, integration of the acetate groups

on the sugar to the Boc group on lysine is 6:9 which is consistent with the desired bis-

galactose product.
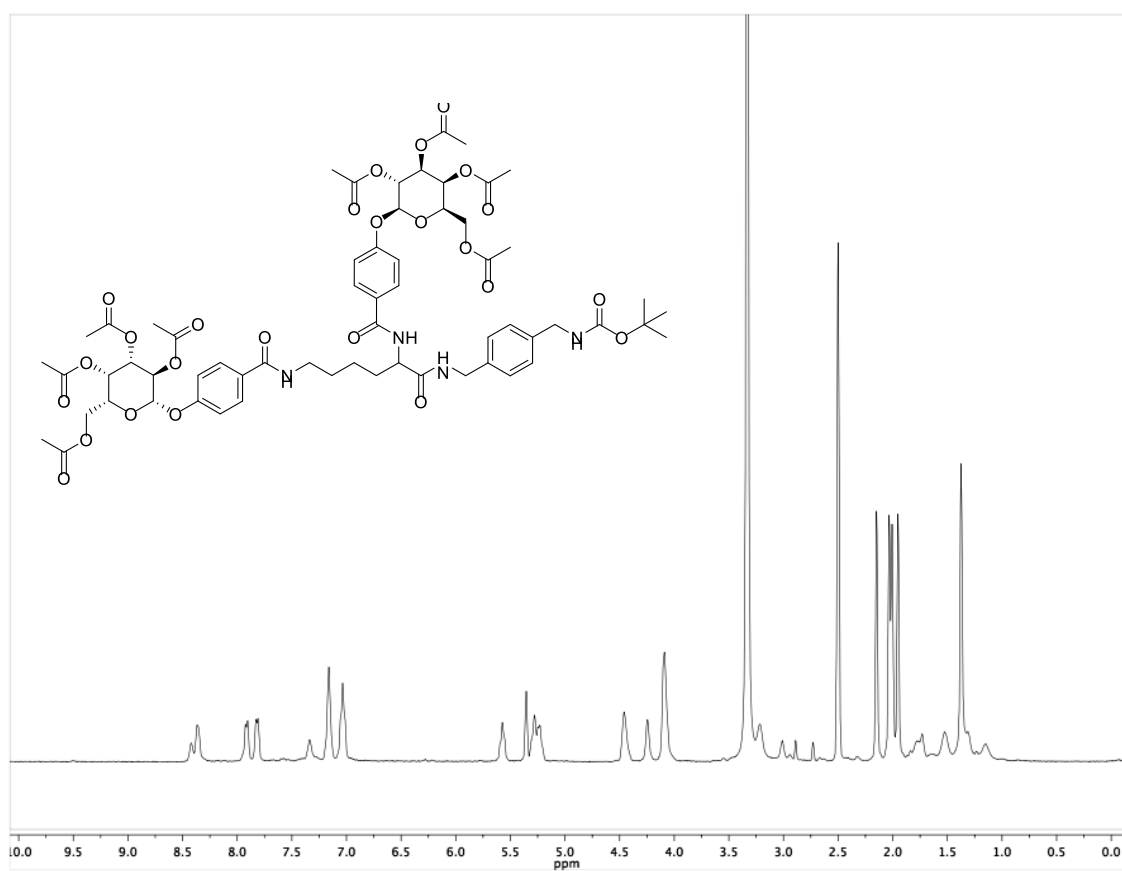
Figure 6. H-NMR of bis-gal modified lysine before deprotection.
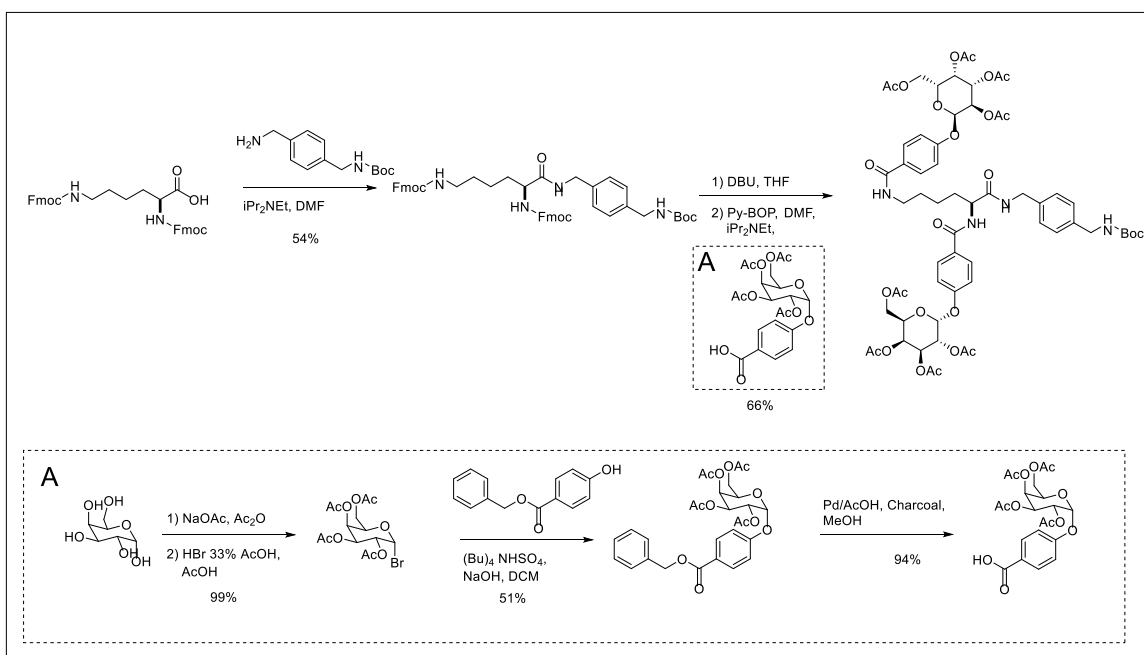
Scheme 4. Synthesis of bis-galactose modified lysine from bis-fmoc lysine. (A) Synthesis of galactose linker for bis-modification.

Having prepared the required bis-galactose modified lysine, one pot coupling to the 6.6kD PS-PEG-OH diblock co-polymer and subsequent acetate deprotection was then attempted (Scheme 4). Success in coupling was achieved with 83% conversion, where unmodified 6.6kD PS-PEG-OH and our desired modified polymer have, to date, proven to be inseparable. While we continue to seek to optimize this process to achieve 100% conversion, the mixture of modified and unmodified polymer does not prohibit our NP assembly, it simply limits the maximum level of surface galactose modification for our NP, in this case to 83% surface modified or less.
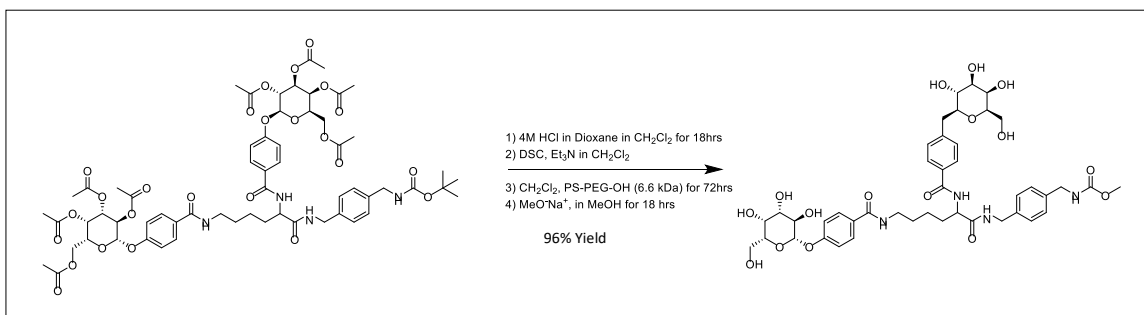
Scheme 5. Synthesis of galactose-modified lysine to PS-PEG

Confirmation of products and determination of % polymer modification was achieved with NMR and mass spectroscopy. The final bis-galactose polymer was too high molecular weight for standard LC-MS measurement. Instead, our products were analyzed by MALDI-MS using methods that would measure compounds of 6kDa to 10kDa in accuracy. It should be noted that the polydispersity of the polymer complicates the analysis significantly by providing a broad peak in the MALDI-MS, consistent with prior studies.
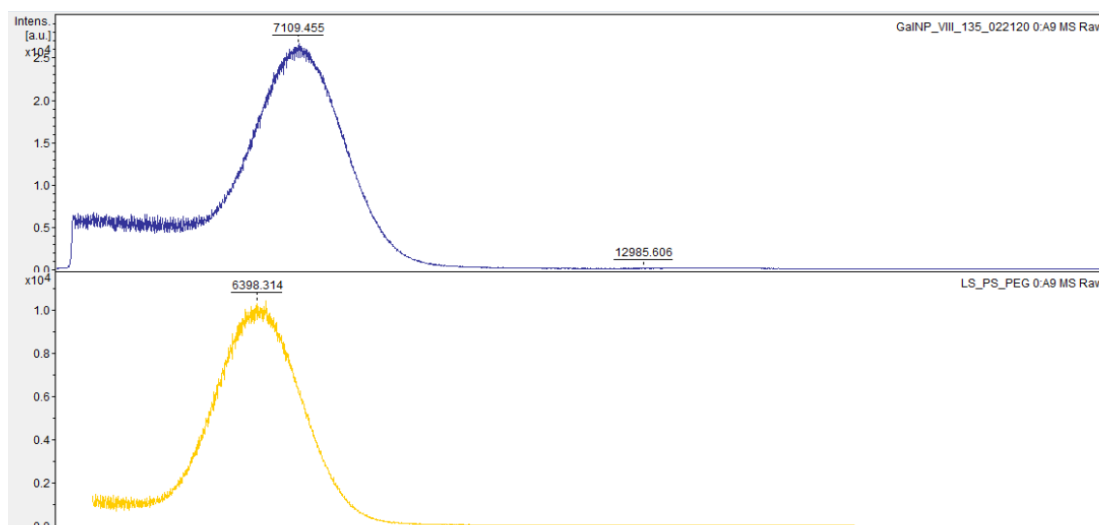
Figure 7. MALDI-MS comparison of 83% modification of galactose per unit polymer (6.6 kDa) (blue) to pure unit polymer (6.6 kDa) (yellow).

To provide a measure of the % polymer modification the delta, or difference between the size seen in the MALDI-MS unmodified and modified polymer peak was measured. This delta value represents a molecular weight difference of 711.141 g/mol between unmodified PS-PEG (6.6kDa) and bis-galactose modified PS-PEG. This can be compared to the theoretical delta value calculated to be 856.88 g/mol to provide our approximation of 83% modification of the polymer. Moreover, MALDI-MS allows for more accurate measurement of our PS-PEG (nominally 6.6kDa per commercial vendor (Polymer Source Inc.) specifications), where unmodified PS-PEG was found to be polydisperse and centered at 6398.314 g/mol by our MALDI-MS measurements. Importantly, the discrepancy between the predicted average mass of the unmodified polymer at 6.6kD and the observed mass of ~6.4kD would not change our calculation of % sugar modification as this is achieved by determination of a delta value prior and after conjugation as described above.

6.3 Evaluation of biological activity with 60% modified galactose nanoparticles.   Our second-generation nanoparticles or, bis-galactose modified nanoparticles, were evaluated for bacterial biofilm formation using crystal violet assay procedures previously described in our first-generation mono-modified nanoparticle. This assay observed a potent dose-dependent inhibition of biofilm formation with our surface-modified Gal-nanoparticle samples up to 60% modification (Figure 8). Inhibition of biofilm formation was noted at D-galactose concentrations above 2.29 μM in the 60%-surface-modified nanoparticle samples. To confirm that the biofilm inhibitory activity observed was not due to growth inhibition by the nanoparticle samples evaluated, we collected growth curve data for PAO1 by monitoring OD_{600}

23

(Figure 9). We determined that at higher concentrations, above 2.29 μM, inhibition of growth would occur. The resulting potency for biofilm inhibitory effect of our 60% bis-galactose-modified nanoparticles proved to be about 33 times more potent than our previously described 100% mono-galactose-modified nanoparticles, which achieved inhibition at concentrations as high as 75.8 μM.
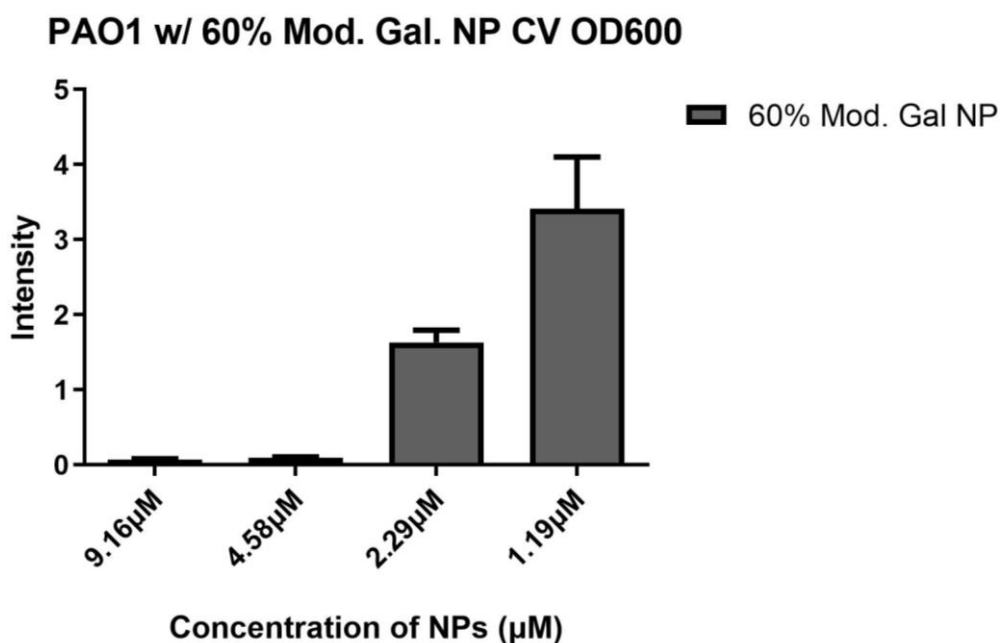
Figure 8. Crystal Violet endpoint assay with P. aeruginosa strain PAO1 and 60% modified bis-galactose-polymer nanoparticles at a 2-fold dilution at 48 hours. All data points are described as the mean of triplicate measurements with error bars representing the standard deviation.
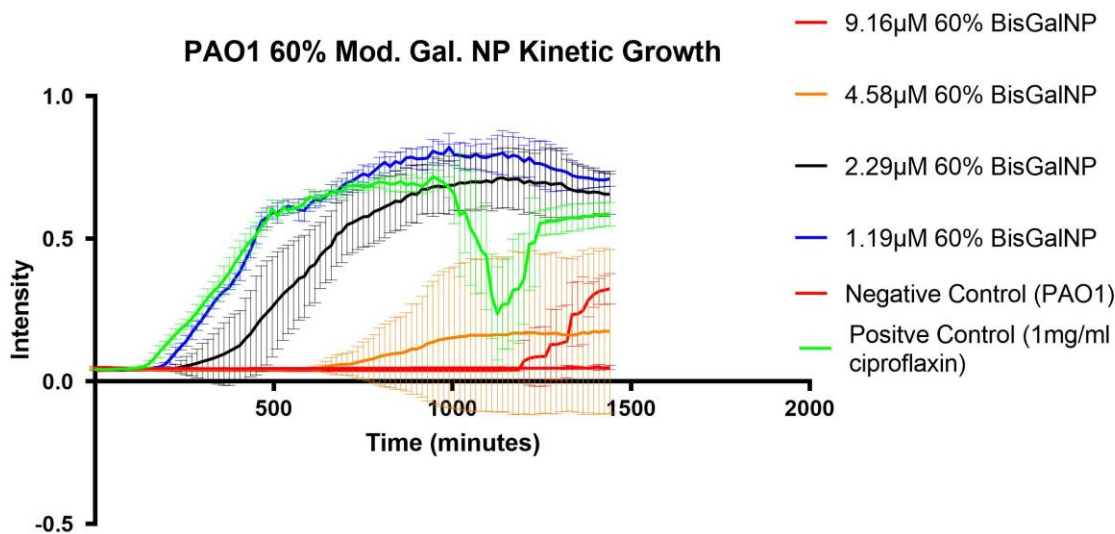
Figure 9. Growth inhibition assay with p. aeruginosa strain PAO1 and concentration curve of 60% modified bis-galactose-polymer nanoparticles at a 2-fold dilution. All data points are described as the mean of triplicate measurements with error bars representing the standard deviation.

6.4 Synthesis of tetra-galactose modified PS-PEG. A synthetic route was proposed in order to couple four galactose sugars per unit PS-PEG. Our previously used sugar, bis-galactose-lysine-diamine, could be added twice to a linker with two available sites. This would allow for two of our lysine-sugars to be added to one-unit PS-PEG, thus having four galactose sugars per polymer. A linker material was selected, cyanuric chloride or TCT, as a prominent candidate for bis-coupling to our previous lysine-sugar.
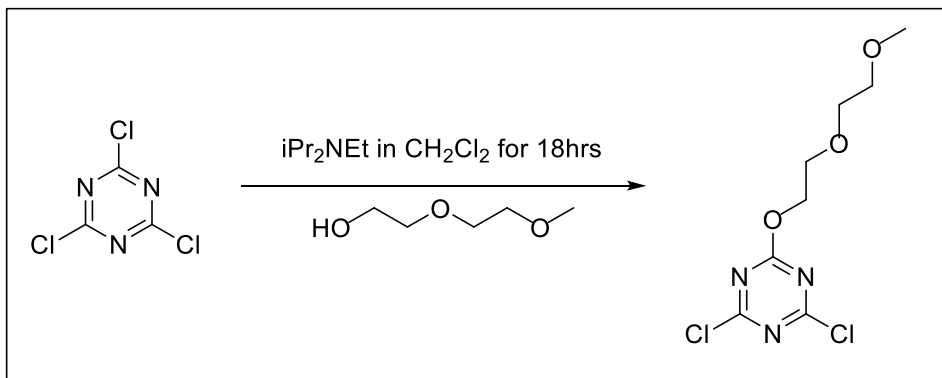
Scheme 6. Synthesis of cyanuric chloride (TCT) coupled to Diethylene Glycol Monomethyl Ether.

6.5 Confirmation of di-chlorotriazine PS-PEG. Synthesis of TCT-PS-PEG presented the first challenge to achieving tetra-galactose modification. A slew of optimization reactions with TCT and a test polymer, Diethylene Glycol Monomethyl Ether, were performed in order to achieve the di-chlorotriazine PS-PEG product. Under mildly basic condition for 18hrs eludes the di-chlorotriazine PS-PEG product. Confirmation of product was optimized by examining di-chlorotriazine Diethylene Glycol Monomethyl Ether products due to their significantly reduced molecular weight. by examining Carbon NMR spectrums, we concluded a shift from the starting material, TCT, single peak at δ172, which are for the 3 carbons in TCT. When the C-NMR of product is examined, there is one new peak that shows up at δ171. The new peak is shorter and lower providing to us that Diethylene Glycol Monomethyl Ether was bound only once to TCT. We can apply this interpretation to other polymers coupling to TCT including our desired TCT-PS-PEG product with 6.6kDa PS-PEG.
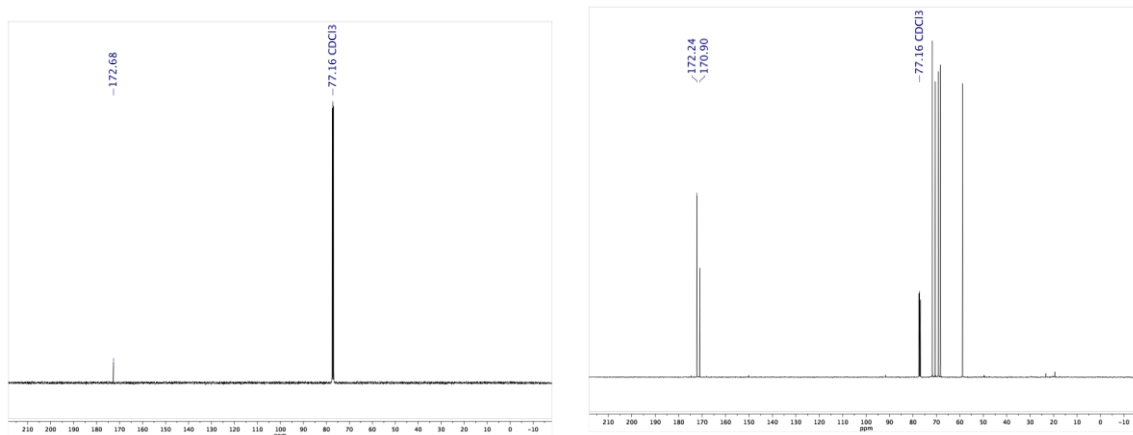
Figure 10. H-NMR of unreacted diethylene glycol monomethyl ether (Left), reacted diethylene glycol monomethyl ether with TCT (Right)

The 6.6kDa PS-PEG coupling to TCT was achieved using reaction conditions optimized with Diethylene Glycol Monomethyl Ether with TCT. As expected, we could conclude our product was achieved by C-NMR by the difference of carbon peaks at δ172 and δ171.
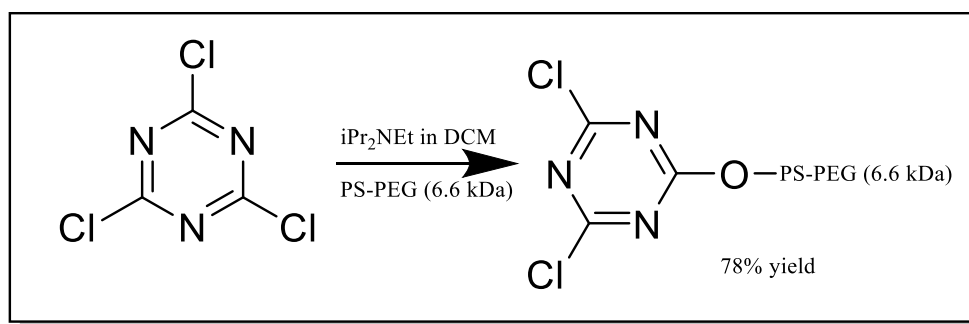
Scheme 7. Mechanism of PS-PEG-OH (6.6kD) coupling to TCT.
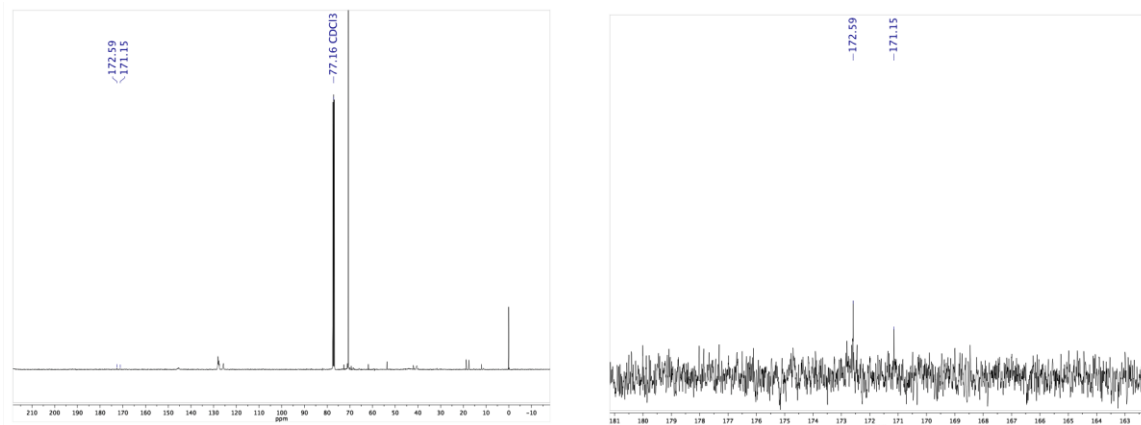
Figure 11. C-NMR of TCT reacted with PS-Peg-OH (6.6kD), where peaks at δ172 and δ171 represent confirmation of coupling by polar changes in the molecule following PS-PEG attachment.

6.6 Synthesis of tetra galactose-modified di-block co-polymer. In order to make the final product, the bis-galactose-lysine-diamine needed to be reacted with TCT at the other available sites (chlorine leaving groups) on TCT. This step proved to be the most challenging in terms of reaction success and qualification. Liturature on the subject of displacing TCT's chlorines proved to be trivial [45]. However, many cases in liturature seeked to couple low molecular weight molecules to TCT [45]. Our high molecular weight 6.6kDa PS-PEG and bulky bis-galactose-lysine-diamine would prove to likely add to the complication of this coupling. Several attempts to achieve coupling at 80°C were attempted without product. MALDI-MS was used to confirm products, similaraly to how we confirmed our bis-gal-PS-PEG products. In solution, tempurature is thought to increase reactivity at the TCT sites. However, by increasing temperature the polymer could begin to rotatate around itself, which might prevent the lysine from binding to the polymer. Our solution to this problem was to attempt this reaction in a microwave reactor at 70°C. It was anticipated that using a microwave would assist in a better distributed

28

heating of the reaction opposed to traditional oil bath heating. Microwave conditions also allowed to reduce reaction times from 2 days to 2 hours (Scheme 7). This change provided product as confirmed by MALDI-MS (Figure 12).
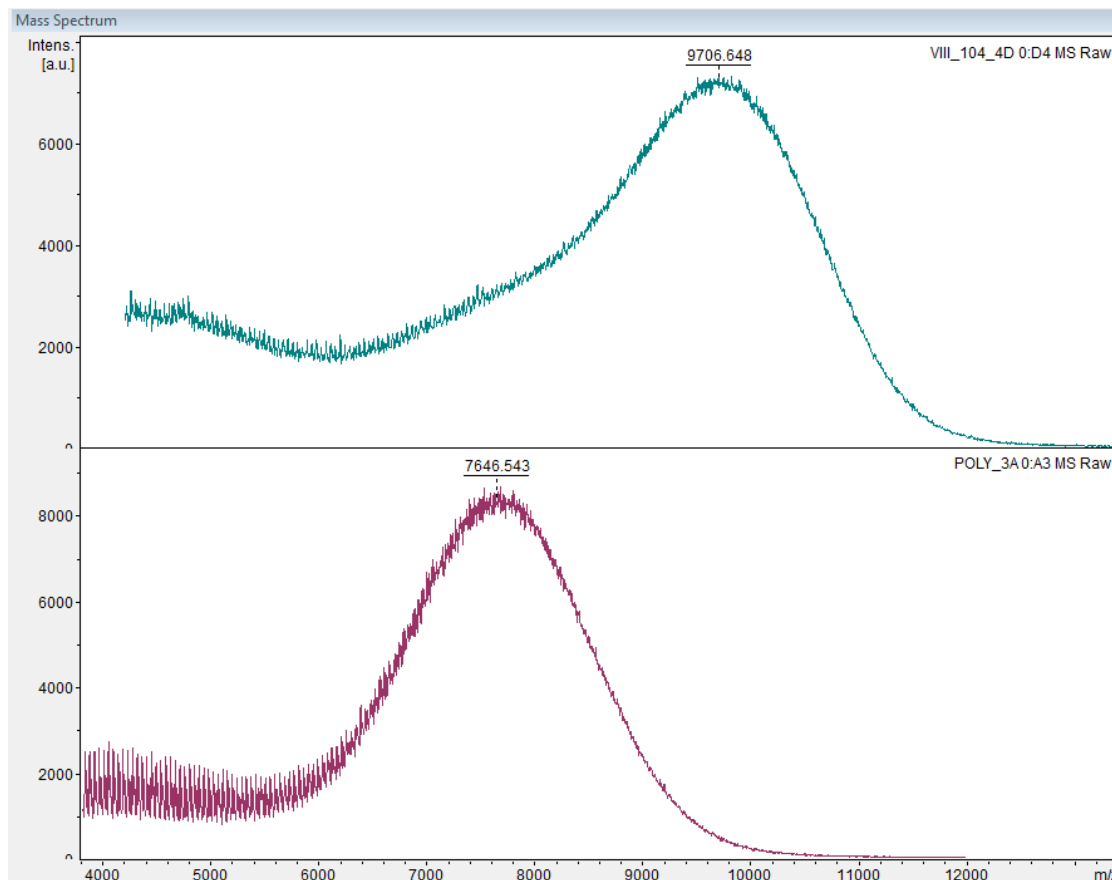
Figure 12. MALDI-MS of TCT tetra-modified galctose product (blue-green) and the starting material PS-PEG-OH (7.6 kDa) in (purple).

Finalizing the sythnesis required acetate deprotection of our fully coupled product. To carryout this reaction we attempted basic conditions in NaOMe/MeOH. The resuting product lead to decoupling of poylmer from our TCT-lysine-sugar complex. Unfortunently, reproducablity of this product was unsuccessful due to instumental problems and our TCT nanoparticles are still under development.
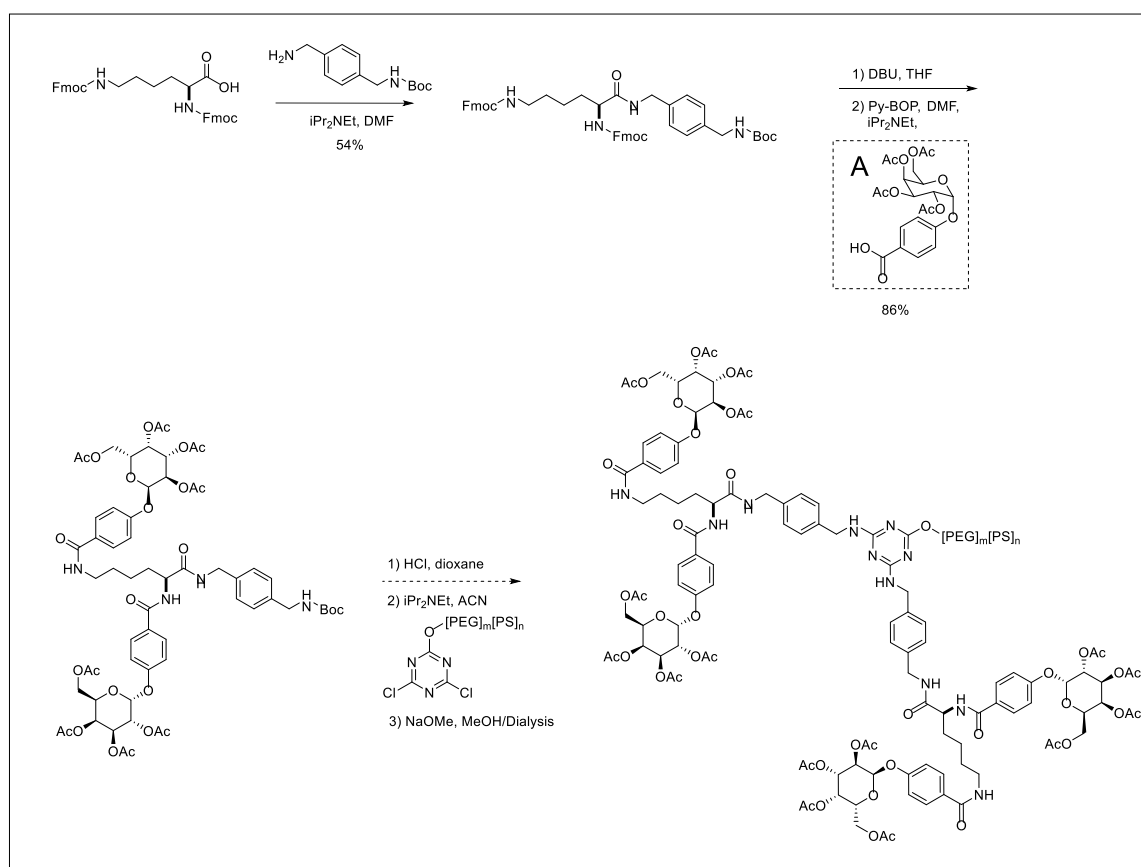
Scheme 8. Synthesis of tetra galactose-modified polymer for nanoparticle assembly.

7. Discussion

Bis-modification of PS-PEG with galactose provided an increase of potency at 60% modification eluding the possibilities of future bis modified polymeric nanoparticles of up to 100% modification. However, synthetic goals are challenged by increasing modification with tetra-modified PS-PEG with galactose. A new synthetic scheme using a lysine-on-lysine was developed due to synthetic challenges seen in our TCT preparation (Scheme 8). Lysine, would act as a TCT substitute due to its function to have 3 sites of coupling. Moreover, discovery in how to couple lysine had already been optimized in our previous analogs with coupling of a benzyl-diamine moiety. Preliminary work on this synthetic route provided crude products.

8. Conclusion

The results of our 60% bis-galactose modified nanoparticles provided a 33-fold increase in potency compared to our first generation nanoparticles in preliminary bacterial assay studies. These results suggest that further modification would provide substantially more potent nanoparticles against *P. aeruginosa*. Further bacterial assay studies are expected to provide decreased toxicity and improved biofilm growth inhibition. However, synthetic challenges have proven to be a crux before determining the specific activity of increased galactose surface modification in *in vitro* studies.

Chapter 3

Synthesis of Fucose Modified Polymers

9. Introduction

Our focus on D-galactose modified sugars provided strong evidence to support their binding and affinity to LecA. However, biofilm formation is also regulated by LecB. LecB binding had yet been evaluated due to lectin binding interaction to L-fucose. To examine LecB specificity, L-fucose surfaced-modified NPs were necessary for our objectives. We hypothesized a similar scaffold of sugar-polymer to be a potent molecule for interaction upon NP formation. These scaffolds, include both Lectin B specify and increased sugar valency. In LecA targeted, we modified each block copolymer with a single sugar molecule. In LecB targeted, we aimed to modify each polymer with two sugars using lysine as a linking molecule.

10. Results

10.1 Synthesis of bis fucose-modified di-block co-polymer using lysine.

Designing LecB targeted NPs began with an isoxazole linker synthesis (Scheme 9). This linker was chosen from a number of different linkers that provide increased affinity for LecB when conjugated with fucose [20]. A linker also provides us with opportunity to terminate our linker-sugar with a carboxylic acid. This functionality allows for easy amide formation for our suggested bis or tetra modified species. Specifically, we examine amide formation on amines present on lysine. Lysine, having two amines, could be functionalized with two sugar molecules through this hypothesized synthetic pathway.
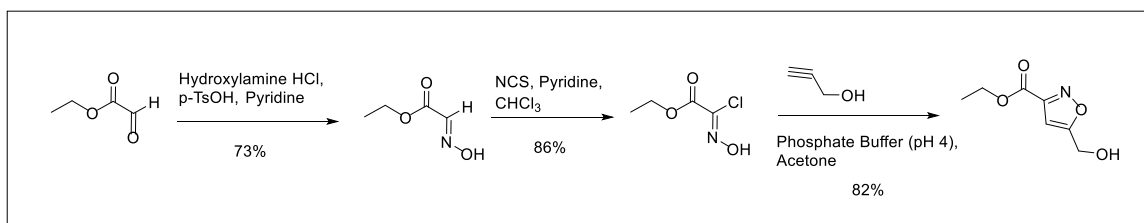
Scheme 9. Synthesis of LecB linker synthesis starting with ethyl glyoxylate.

Ethyl glyoxylate is reacted with hydroxylamine in preparation for cyclization at seventy-three percent yield. The key moiety in this linker synthesis is an isoxazole ring, which likely contributes to the increased affinity seen in previous studies [46]. Prior to cyclization, N-chlorosuccinimide is reacted on the alkene giving it a chlorine necessary for its leaving group probability upon reaction with an alkyne in a Diels-Alder-like cyclization. This step is performed at 82 percent yield. It was suggested at this point addition of sugar and subsequent reduction of the ethyl ester would be achieved, however, this led to degradation, particularly upon LiOH reduction (Scheme 10).
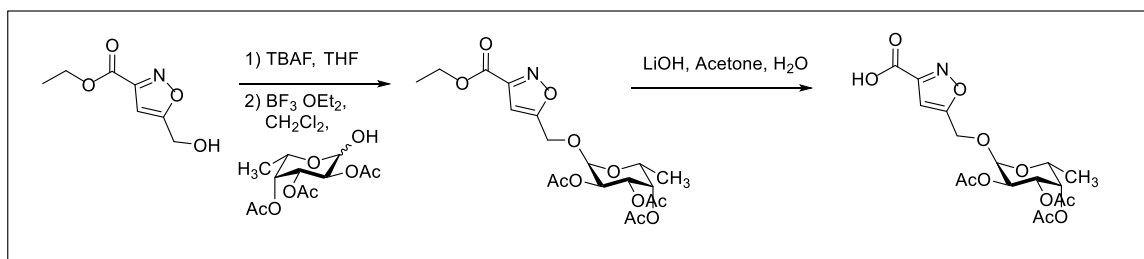
Scheme 10. Synthesis of LecB linker coupling with L-Fucose.

33

To rework the synthesis, we proposed to protect the alcohol on the linker

molecule and immediately perform reduction of the ethyl ester before addition of fucose.

This would reverse our couplings, meaning we will couple the acid to lysine prior to

sugar coupling (fig mole). TBDPS (tert-Butyldiphenylsilyl) protection was used, since it

contained two large aromatic rings that could be easily detected by UV supported flash

purification. Synthesis was achieved using our previous reaction, however, before

cyclization with propargyl alcohol, the hydroxyl was protected with TBDPS. Following

reduction of the ethyl ester, coupling to lysine was performed with HATU reagent using

our diamine terminated lysine following our previous preparation. Unfortunately, upon

TBDPS deprotection with TBAF degradation occurs. Several workarounds were

examined including differing acid deprotection reagents and modifying protection

groups, but none provided product.
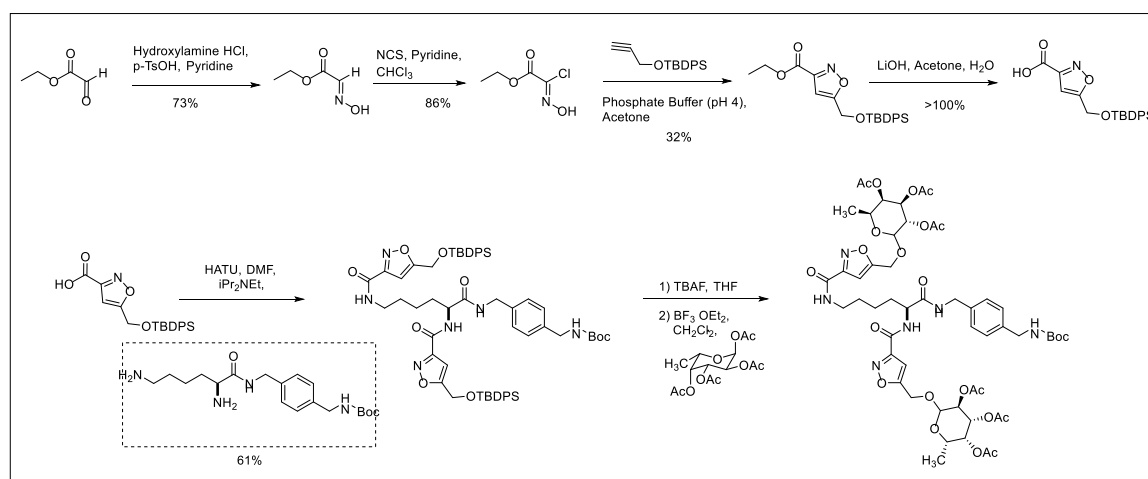
Scheme 11. Synthetic scaffold of bis fucose-modified lysine using lysine derivatives.

It was determined that our isoxazole linker could be replaced by another linker; one that we were familiar with in our galactose synthesis. By including our pervious hydroxyl benzyl acid linker as a LecB linker we can still achieve increased potency in fucose-lectin binding. We completed synthesis as per our previous procedure, but now with L-fucose instead of D-Galactose (Scheme 12).
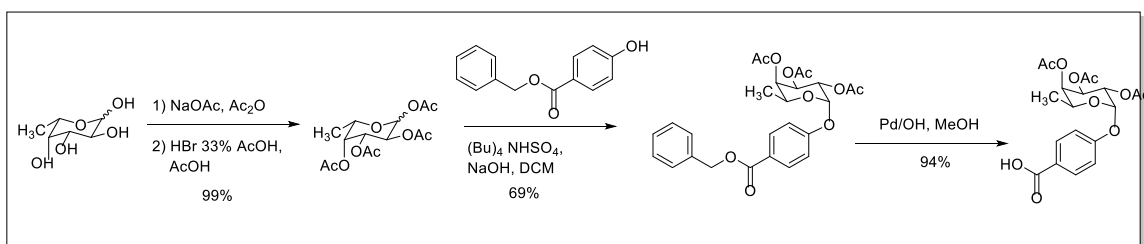
Scheme 12. Revised synthesis of LecB linker synthesis starting with benzyl benzoate.

For our LecB targeted nanoparticles, we took our focus directly to sis-modified nanoparticles. Our discovery into a reproducible lysine product would provide to useful to bind our modified fucose to our block co-polymer. Following the synthesis used in LecA, we were able to achieve 100% modified nanoparticles with bis-fucose. This also allowed us insight into the multi-step process, specifically, we determined several issues regarding our final steps. It was determined that in some cases severe degradation of the molecule occurs after sodium hydroxide deprotection of acetate groups on our sugars. In this case, where we achieved product at 100% modification, where conditions involved the removal of the atmosphere from exposer to the reaction vessel. MALDI-MS confirmed that the product had been achieved by providing a difference or delta value

between the maximum intensity of the un-modified PS-PEG (6.6 kDa) and the bis-fucose

modified PS-PEG (6.6kDa) at a value of 871.054 g/mol. (Figure 13). This can be

compared to the calculated molecular weight, 866.92 g/mol, of our bis-fucose benzyl-

diamine lysine, which accounts for the only difference (delta) between the two

compounds. This comparison confirms that we successfully modified PS-PEG (6.6kDa)

in ~100% conversion.
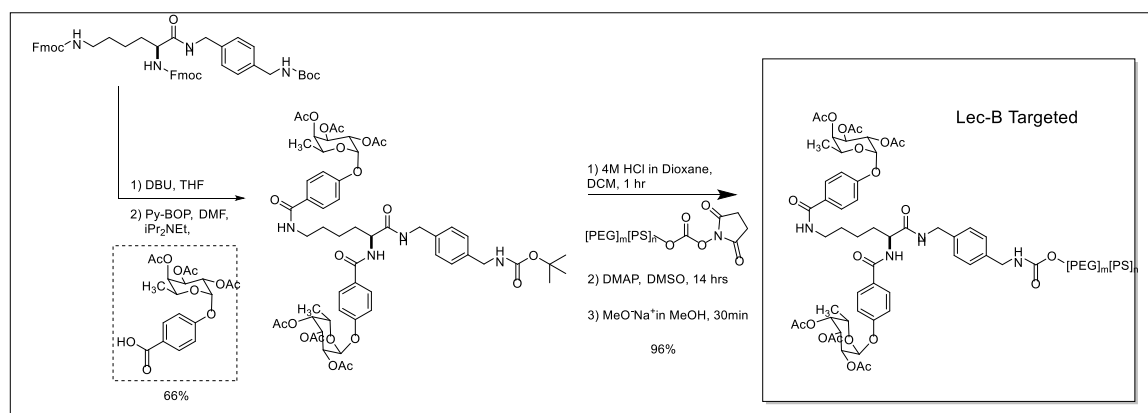
Scheme 13. Mechanism of LecB fucose-linker coupling with lysine and subsequent
coupling with PS-PEG 6.6kDa.
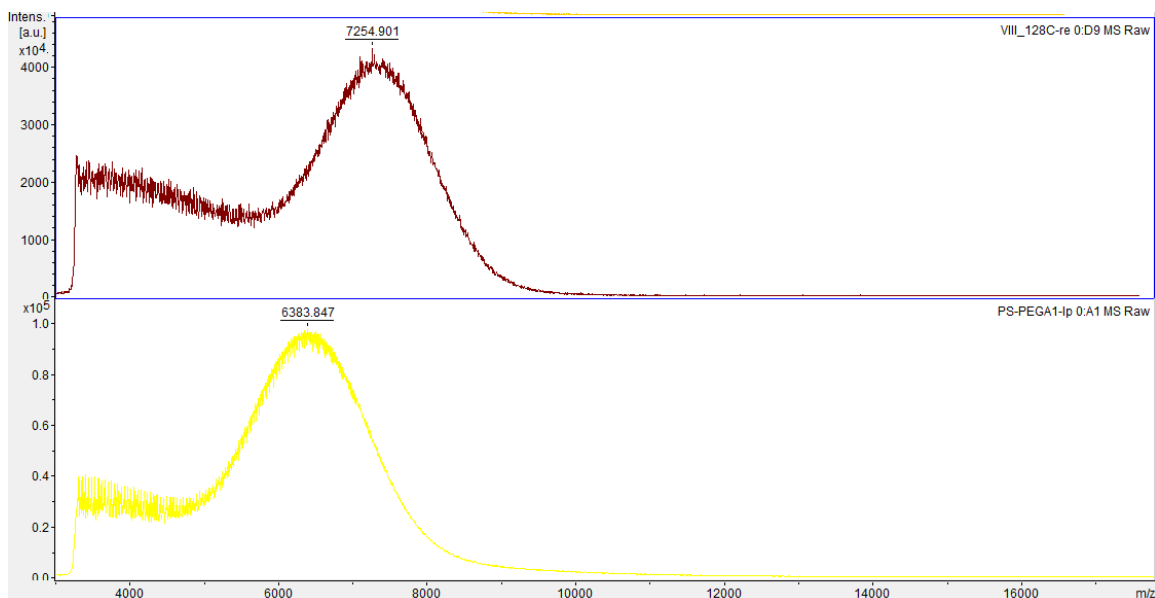
Figure 13. MALDI-MS of 100% modification of PS-PEG (6.6 kDa) with bis-fucose lysine (maroon) compared to non-modified PS-PEG (6.6kDa).

10.2 Nanoparticle precipitation of bis-modified fucose polymers. Nanoparticle formation was preformed using a mixing block to precipitate nanoparticles of fucose surface modification at 100%, 50%, 25% and 0%. This is achieved using mixtures of modified PS-PEG and un-modified PS-PEG at the corresponding ratios. Procedure for precipitation is followed as conducted in section 2.2. In addition to section 2.2, the precipitated nanoparticles undergo a 30-minute desiccation under reduced pressure on a rotary evaporator followed by a two-hour desiccation in a chamber under reduced pressure to remove any THF present in the sample from flash precipitation. This process ensures that the nanoparticle solution will not have THF present during bacterial assay studies, which could affect the outcome due to toxicity. Nanoparticles are then analyzed for particle size and polydispersity by dynamic light scattering (DLS) (Figure 14). DLS data provided size distribution in diameter of 50-200 nm.

37
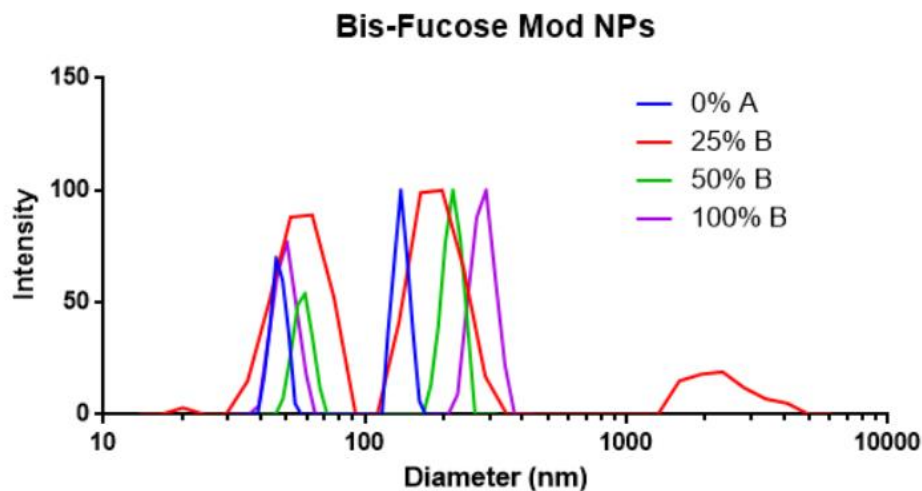
Figure 14. Dynamic light Scattering data for bis-fucose surface modified nanoparticles at 100%-0% surface modification.

10.3 Evaluation of biological activity with bis fucose-modified nanoparticles.

Biological activity of Fucose modified nanoparticles was provided in several bacterial

assay studies. To determine effective concentration against biofilm formation of

P.aeruginosa, a crystal violet assay (CV assay) was developed (Figure 15). A kinetic

growth assay was also provided to compare toxicity effects to inhibition. Comparing

biofilm inhibition to growth inhibition can determine which concentrations of biofilm

was inhibited where growth was not. It was determined fucose modified nanoparticles

inhibit biofilm at 4.19 μM in our crystal violet endpoint assay (figure 15). Concentrations

above 8.38 μM lead to growth inhibition in *P.aeruginosa* PAO1 (figure 16). A 18-fold

increase in potency is achieved compared to mono-galactose modified nanoparticles, which inhibit biofilm up to 75.8 μM.

Concentrations of 25μL (8.38 μM) to 50μL (16.75 μM) of 100% with 100%-bis Fucose surface-modified nanoparticles was determined to inhibit growth of *P. aeruginosa* PAO1 by monitoring OD600 intensity. However, biofilm formation was inhibited at a concentration of 12.50 μL (4.19 μM) and concentrations of 4.19 μM and below provided growth in PAO1. Fucose surface-modified nanoparticles at a concentration of 4.19 μM with biofilm inhibition can be compared to 100% mono modified galactose nanoparticles biofilm inhibition concentration of 75.8 μM, which provides a 18-fold decrease in the concentration necessary to inhibit biofilm formation against *P. aeruginosa*.
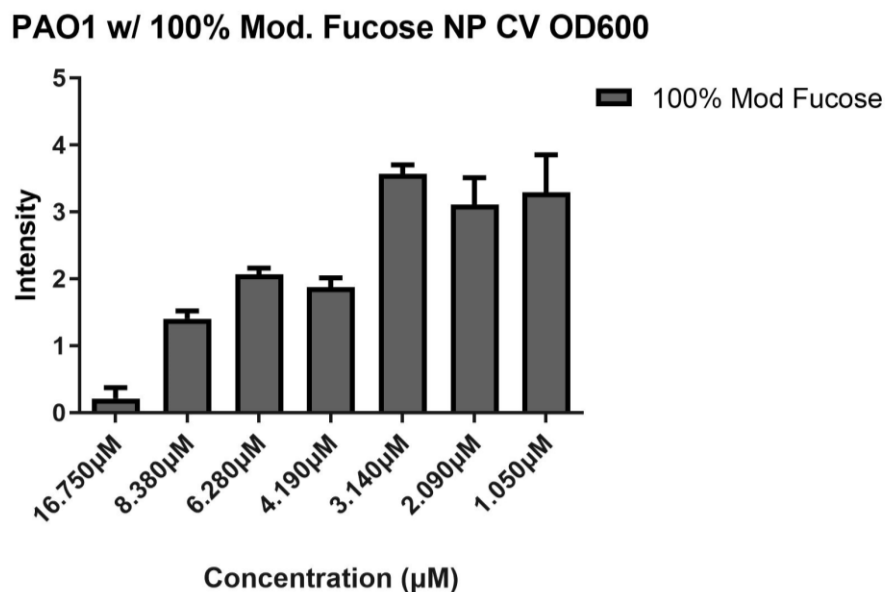
Figure 15. Inhibition of *P. aeruginosa* PAO1 biofilm formation based on the crystal violet assay. Surface-modified bis-Fucose-NP samples are described based on relative concentration of L-fucose on the nanoparticle surface. All data points are described as the mean of triplicate measurements with error bars representing the standard deviation.
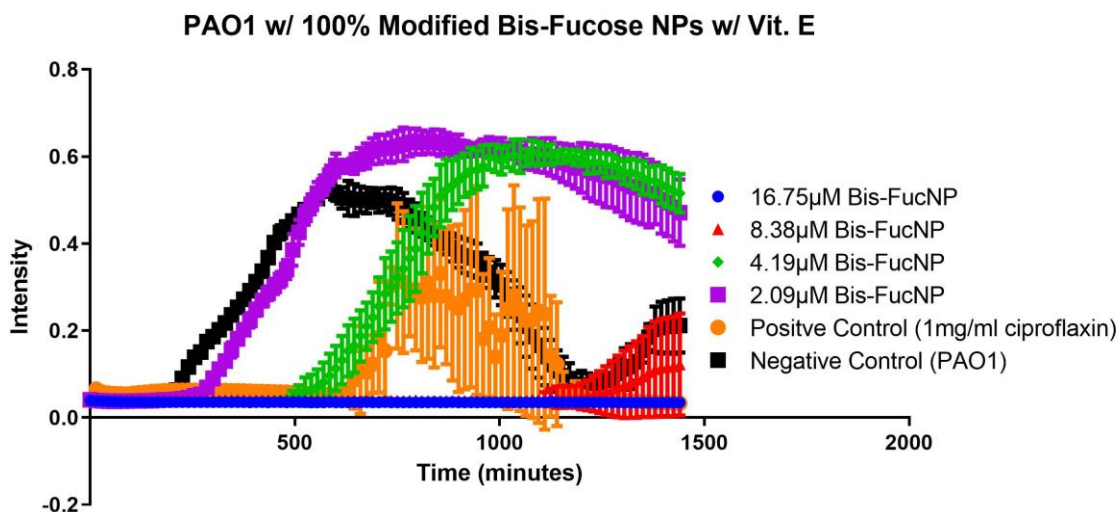
Figure 16. Evaluation of *P. aeruginosa* PAO1 growth by monitoring OD$_{600}$ with 100%-bis-L-Fucose-surface-modified nanoparticles. No significant growth inhibition is observed with 100%-modified Fucose-NP at concentrations at or below 4.19 µM. Growth inhibition was noted at concentrations above two-fold higher at 16.75 µM. Error bars represent standard deviation of triplicate analysis.

11. Discussion

Fucose modification on the surface of polymeric nanoparticles provides a distinctive binding interaction when compared to galactose. L-Fucose, specific to Lec-B binding, proves to be effective in inhibition of biofilm in preliminary bacterial assay studies with a minimum inhibition concentration of 4.19 µM. Bis-modification could be the cause for the decreased effective inhibition concentration, since a two-fold increase in the number of sugars is modifying the surface of the nanoparticle when compared to mono-modified galactose nanoparticles. A 18-fold increase in potency from our bis-fucose modified nanoparticles could be compared to a 33-fold increase in potency seen in 60% bis-modified galactose nanoparticles, which could provide evidence that our Lec-A targeted nanoparticles are more effective. However, nanoparticles could be precipitated in a 1:1 ratio with Lec-B and Lec-A specific surface modification or fucose and galactose

modification, respectively. Combination of lectin targeting could provide more effective specific targeting, increased potency and increased biofilm growth inhibition.

12. Conclusion

Synthesis of Lec-B targeted nanoparticles proved to be more effective in achieving bis-modification when compared to Lec-A specific targeting for *P. aeruginosa*. However, future analogs could provide could provide to be more difficult as we approach tetra modified synthetic goals. Overall, a 4.19 μM biofilm inhibition concentration is a exciting starting point for the evaluation of future analogs.

Chapter 4

Supporting Information

13. Materials and Methods

13.1 General experimental. Unless otherwise noted, all reactions were performed in flame-dried glassware under an atmosphere of nitrogen or argon using dried reagents and solvents. All chemicals were purchased from commercial vendors and used without further purification. Anhydrous solvents were purchased from commercial vendors.

Flash chromatography was performed using standard grade silica gel 60 230-400 mesh from SORBENT Technologies or using a Biotage Flash Purification system equipped with Biotage SNAP columns. All purifications were performed using gradients of mixtures of ethyl acetate and hexanes. Analytical thin-layer chromatography was carried out using Silica G TLC plates, 200 μm with UV_{254} fluorescent indicator (SORBENT Technologies), and visualization was performed by staining and/or absorbance of UV light.

NMR spectra for small molecules were recorded using a Varian Mercury Plus spectrometer (400 MHz for ^{1}H-NMR; 101 MHz for ^{13}C-NMR). Chemical shifts are reported in parts per million (ppm) and were calibrated according to residual protonated solvent. Mass spectroscopy data was collected using an Agilent 1100-Series LC/MSD Trap LC-MS or a Micromass Quattromicro with a Waters 2795 Separations Module LC-MS with acetonitrile containing 0.1% formic acid as the mobile phase in positive ionization mode. Small molecule purity was determined on an Agilent 1100 series equipped with a Phenomenex Kinetex 2.6 µm C18-UPLC column using a gradient of water to acetonitrile with 0.1% TFA.

All final compounds were evaluated to be of greater than 90% purity by analysis of ^{1}H-NMR, ^{13}C-NMR, and/or analytical HPLC.

13.2 Synthesis of D-galactose-modified polymers. (2*S*,3*R*,4*S*,5*S*,6*R*)-6-(acetoxymethyl) tetrahydro-2*H*-pyran-2,3,4,5-tetrayl tetraacetate, 2. D-galactose (5.00 g, 27.75 mmol) was dissolved in acetic acid (185 mL, 0.15 M) at room temperature. Acetyl bromide (16.40 mL, 222.02 mml) was added and the mixture was allowed to stir for 1 hour. The resulting solution was washed with toluene (2x, 40 mL), dried over sodium sulfate, and concentrated to dryness. The residue was purified by flash chromatography using a gradient of hexanes to EtOAc to provide (2*S*,3*R*,4*S*,5*S*,6*R*)-6-(acetoxymethyl) tetrahydro-2*H*-pyran-2,3,4,5-tetrayl tetraacetate. Characterization data was consistent with a commercial sample of this compound.

(2*R*,3*S*,4*S*,5*R*,6*S*)-2-(acetoxymethyl)-6-(4-((benzyloxy)carbonyl)phenoxy)tetrahydro-2*H*-pyran-3,4,5-triyl   triacetate,   4. (2*S*,3*R*,4*S*,5*S*,6*R*)-6-(acetoxymethyl)tetrahydro-2*H*-pyran-2,3,4,5-tetrayl tetraacetate, **2** (2 g, 5.12 mmol) was dissolved in dichloromethane (10 mL, 0.5 M) at room temperature. Hydrobromic acid (33% in AcOH, 1.485 mL) and acetic acid (3.015 mL, 1.14 M) were added and the mixture was allowed to stir. After 30 minutes, the solution was diluted with 50 mL of DCM, washed with sodium bicarbonate, dried with sodium sulfate, and concentrated to dryness. The residue (2 g) was re-dissolved in DCM (30 mL, 1.5 M) and treated with benzyl-4-hydroxybenzoate, **3** (2.34 g, 10.03 mmol), tetrabutylammonium hydrogensulfate (1.74 mg, 5.12 mmol), and 0.5 M sodium hydroxide (10 mL, 0.5 M). The biphasic mixture was allowed to stir overnight at room temperature, was diluted with DCM and acidified with 1M HCl, extracted with DCM (3 x 50mL), dried over Na$_2$SO$_4$, and

concentrated to dryness. The residue was purified by flash chromatography using a gradient

of hexanes to EtOAc to provide (2*R*,3*S*,4*S*,5*R*,6*S*)-2- (acetoxymethyl)-6-(4-

((benzyloxy)carbonyl)phenoxy) tetrahydro-2*H*-pyran-3,4,5-triyl triacetate, **4** (1.006 g,

1.848 mmol, 40.76%). ^{1}H NMR (400 MHz, CDCl$_3$) δ^{1}H NMR (400 MHz, CDCl$_3$) δ 7.96

(d, *J* = 8.9 Hz, 2H), 7.40–7.22 (m, 5H), 6.95 (d, *J* = 8.4 Hz, 2H), 5.48–5.37 (m, 2H), 5.27

(s, 2H), 5.11–5.01 (m, 2H), 4.20–3.95 (m, 3H), 2.11 (s, 3H), 1.98 (s, 6H), 1.94 (s, 3H). ^{13}C

NMR (101 MHz, CDCl$_3$) δ 170.44, 170.30, 170.19, 169.44, 165.88, 160.46, 136.19,

131.84, 128.72, 128.37, 128.25, 125.14, 116.30, 98.93, 71.39, 70.84, 68.59, 66.93, 66.76,

66.76, 61.50, 20.82, 20.79, 20.76, 20.69, 0.12. ESI-MS: predicted for C$_{28}$H$_{31}$O$_{12}$ [M+H]$^+$

559.544, observed, 559.569.

4-((((2*S*,3*R*,4*S*,5*S*,6*R*)-3,4,5-triacetoxy-6-(acetoxymethyl)tetrahydro-2*H*-pyran-2-

yl)oxy)benzoic   acid,   5.   (2*R*,3*S*,4*S*,5*R*,6*S*)-2-(acetoxymethyl)-6-(4-

((benzyloxy)carbonyl)phenoxy)tetrahydro-2*H*- pyran-3,4,5-triyl triacetate, **4** (0.719 g,

1.320 mmol) was dissolved in methanol (6.6 mL, 0.2 M) and palladium on carbon (10%,

16 mg, 0.1 mmol) was added to the reaction flask at room temperature. Hydrogen was

added via balloon and the reaction was stirred overnight at room temperature. The residue

was separated by vacuum filtration washing with methanol to yield 4-((((2*S*,3*R*,4*S*,5*S*,6*R*)-

2,3,4,5-tetrahydroxy-6-(hydroxymethyl)tetrahydro-2*H*-pyran-2-yl) methoxy)benzoic acid,

5 (571.2 mg, 1.219 mmol, 61.85%). ^{1}H NMR (400 MHz, CDCl$_3$) δ 8.05 (d, *J* = 8.3 Hz,

2H), 7.03 (d, *J* = 8.3 Hz, 2H), 5.57–5.43 (m, 2H), 5.20–5.07 (d, *J* = 51.1 Hz, 2H), 4.28–

4.06 (d, *J* = 84.7 Hz, 3H), 2.19 (s, 3H), 2.06 (s, 6H), 2.02 (s, 3H). ^{13}C NMR (101 MHz,

CDCl$_3$) δ 171.98, 171.91, 171.38, 171.22, 161.55, 132.97, 132.72, 117.02, 115.98, 99.36,

72.27, 72.16, 70.02, 68.67, 62.60, 49.00, 24.74, 20.69, 20.60, 20.54, 20.50, 20.49, 13.93. ESI-MS: predicted for $C_{21}H_{24}O_{12}Na$ [M+Na]$^+$ 491.401, observed, 491.477.

PS-*b*-PEG-Galactose, 1. To a room temperature solution of 4-((((2*S*,3*R*,4*S*,5*S*,6*R*)-2,3,4,5-tetrahydroxy-6-(hydroxymethyl)tetrahydro-2*H*-pyran-2-yl) methoxy)benzoic acid, **5** (20.5 mg, 0.068 mmol) in DMF (340uL) was added (Benzotriazol-1-yloxy)tris(dimethylamino)phosphonium hexafluorophosphate (30.1 mg, 0.068 mmol) and the mixture was allowed to stir for 5 minutes before the addition of PS-*b*-PEG-NH₂ (150 mg, 0.023 mmol, 6.6 kD, prepared from PS-*b*-PEG-OH as previously described [18]). The resulting solution was stirred at room temperature overnight. The reaction was quenched by the addition of water (1 mL) and EtOH (1 mL), and loaded into a 3.5 kD MWCO dialysis cassette (Pierce^{TM} Slide-A-Lyzer^{TM} G2, Thermo Scientific). The mixture was dialyzed into water for 12 h, at which time the dialysis cassette was transferred to a fresh solution of water and further dialyzed for an additional 12 h. After dialysis, the retained solution was lyopholyzed to provide PS-*b*-PEG-galactose, 1, as a white powder (153.6 mg, quantitative). The product was characterized by MALDI-MS (Bruker MicroFlex LFR MALDI-TOF) in positive linear detection mode using a matrix of dithranol:polymer of 1:1 evaporated from DCM onto a polished steel target. Collected spectra were analyzed with the Flex Analysis software (Bruker); the unmodified PS-*b*-PEG-NH₂ was evaluated in the same manner as a standard. The observed m/z for PS-*b*-PEG-NH₂ was 6212.07, and the observed m/z for PS-*b*-PEG-galactose was 6501.40, consistent with complete polymer modification (anticipated Δ m/z for polymer modification = 282.24).

13.3 Nanoparticle assembly. Nanoparticles with defined levels of surface modification were prepared through flash nanoprecipitation (FNP) as previously described

[18,19,39]. Briefly, PS, vitamin E (VitE), PS-*b*-PEG, PS-*b*-PEG-galactose, and/or PS-*b*-PEG-mannose were dissolved at defined compositions in THF and rapidly micromixed with an equivalent volume of water within a confined impingement jet mixer, manufactured using HDPE (The Inventors Shop, Cinnaminson, NJ, USA), following the specifications provided [40], and diluted tenfold in a water collection bath. Particles with 0–100%-surface-modification of galactose or mannose were prepared using defined combinations of PS-*b*-PEG/PS-*b*-PEG-galactose or PS-*b*-PEG-mannose. Vitamin E was used as the core bulking material in all NP formulations. Particle sizes were assessed with dynamic light scattering analysis (90Plus Particle Size Analyzer, Brookhaven Instruments Corporation). Size distributions were determined with backscattering measurements from 658-nm illumination and displayed as intensity-weighted distributions; 'particle diameter' is the hydrodynamic diameter as calculated by DLS based on the Stokes Einstein equation using instrumental software. The composition of particles formed and particle size characterization data is provided in Table 1.

13.4 Hemagglutination assay. The LecA-induced hemagglutination assay was performed as reported with modifications [20]. LecA (PA-IL) was purchased from Sigma-Aldrich and used as received. Rabbit red blood cells (Innovative Research) at 100% were washed three times with 150 mM NaCl solution then diluted to 5% with NaCl (150 nM) solution. A hemocytometer was used to count the number of red blood cells that were in red blood cell solution and solutions were normalized to 2.94×10^{14} cells/mL. To find the minimal full hemagglutination inhibition concentration for LecA, a serial dilution was performed from a stock solution of 1 mg/ml LecA. Briefly, LecA (15 µl) was diluted into Tris buffer (Tris 20 µM, NaCl 100 mM, CaCl$_2$ 100 µM, pH = 7.5, 35 µl) in 96-well

microtiter V-bottom plates and was subjected to a two-fold serial dilution. Normalized 5% blood solution (10µl) was added to each well and incubated for 30 minutes at room temperature. After incubation, the plate was centrifuged for 1 minute at low rpm. The minimum full hemagglutination inhibition for LecA was found to be 1.2 µg/ml. Further analysis of inhibition of LecA-induced hemagglutination was performed with LecA at 4xHU (4.8 µg/ml). Briefly, 25 µl of each nanoparticle formulation was subjected to a two-fold serial dilution in Tris buffer and LecA was added to a final concentration of 4xHU. The plate was then incubated for 2 hours at room temperature. After incubation, normalized 5% blood solution (10 µl) was added. The plate was then incubated for 30 minutes at room temperature and then centrifuged for 1 minute at low rpm before analysis.

13.5 Crystal violet biofilm inhibition assay. The effect of inhibitors on static biofilm formation was evaluated using the crystal violet staining method with *P. aeruginosa* strain PAO1 [25] following the established procedure [41]. Briefly, overnight cultures of *P. aeruginosa* PAO1 were diluted 1:100 into fresh LB media. Compounds were added at the indicated concentrations in a 96-well microplate before static incubation at 37 °C for 24 hours. After incubation, the plates were thoroughly rinsed to remove planktonic cells and the adherent cells were quantified by staining with crystal violet and measurement of A_{550}. The assay was performed with five replicates for each compound concentration. After exclusion of the highest and lowest absorbance readings the remaining triplicate readings were described as means with error bars representing standard deviations.

13.6 Growth inhibition assay. The effect of nanoparticles on bacterial growth was evaluated with *P. aeruginosa* strain PAO1 [25]. Overnight cultures of *P. aeruginosa* PAO1 were diluted 1:100 into fresh LB media. Nanoparticle formulations/compounds were added

at the indicated concentrations in a 96-well microplate. The plate was placed in a Molecular Devices SpectraMax i3x incubating plate reader set at 37 °C with shaking. Measurement of A_{600} was recorded every 15 minutes for the duration of the experiment. Readings are reported as means with error bars representing the standard deviations of triplicate analyses.

13.7 Fluorescent confocal microscopy. The effect of inhibitors on static biofilm formation was evaluated by confocal fluorescence microscopy with *P. aeruginosa* strain PA14 [25] following the established procedure [42]. Briefly, overnight cultures of PA14-GFP [23] were diluted 1:100 into the designated media. Compounds were added at the indicated concentrations in 96-well microplates with optical grade glass bottoms (Corning) before static incubation at 37 °C for 24 hours. After incubation, the samples were imaged on a Nikon Eclipse TI confocal microscope equipped with a 10X lens. Images were acquired from a central point in each well of the microplate. Each compound concentration was evaluated in duplicate. Image stacks were analyzed using Comstat2 [43, 44].

13.8. Synthesis of tetra-galactose modified polymers.

13.8.1 Mono-Boc diamine. p-xylyldiamine (0.200 g, 1.468 mmol) in DCM at 0°C. triethylamine (0.500 mL, 3.5232 mmol) was added to cold solution. Next, a separate solution of di-tert-butyl pyrocarbonate (0.1282 g, 0.5873 mmol) in DCM was added to the first solution. This reaction was stirred overnight (18hrs) to room temperature (23°C). The reaction was converted in vacuum and redissolved in DCM (30mL) washed with bicarb, brine, dried, concentrated. **7** (0.1318 g, 0.5577 mmol, 95%)

13.8.2 Bis-Fmoc Lysine mono-boc linker. To a solution of bis-fmoc-L-lysine (2.499 g, 4.23 mmol) and mono-boc diamine **7** in DMF, N,N-diisopropylethylamine (3.55 mL, 20.30 mmol) and (Benzotriazol-1-yloxy) tripyrrolidinophosphonium hexafluorophosphate (2.64 g, 5.07 mmol) were added and reaction ran for 4 hours. Reaction was crashed out with water, the white solids were filtered, the white solids were then treated with Methanol and stirred overnight. Ten white solids were filtered out and were kept for further use. (1.8276 g, 2.259 mmol, 53.5%)

13.8.3 Bis-Galactose lysine mono-boc linker. To a solution of bis-fmoc lysine mono-boc linker (0.200 g, 0.2472 mmol) in DMF, 1,8-diazabicyclo[5.4.0]undec-7-ene (0.369 mL, 2.472 mmol) was added. This reaction was stirred at room temperature (23°C) for 30 minutes. Once done, the reaction was treated with 24 mL of diethyl ether and stirred for 5 minutes then placed into the freezer for 30 minutes. The supernatant was removed and the solids were concentrated and used crude (lysine mono-boc linker) without further purification. The crude product (0.2472 mmol) was made into a solution with DMF and modified D-galactose (0.2895 g, 0.6180 mmol) at room temperature (23°C). To this solution, N,N-diisopropylethylamine (0.2153 mL, 1.236 mmol) and (Benzotriazol-1-yloxy) tripyrrolidinophosphonium hexafluorophosphate (0.3216 g, 0.6180 mmol) were added and stirred for 4 hours at room temperature (23°C). Once done, the reaction was quenched with water (50 mL) and vacuum filtered. The white solids were extracted and concentrated to yield product (0.292 g, 0.231 mmol, 93.4%)

13.8.4 Di-chlorotriazine PS-PEG (6.6 kD). To a solution of PS-PEG-OH (6.6 kD) (0.1037 g, 0.01364 mmol) in DCM, trichorotriazine (0.0503 g, 0.2729 mmol) and N,N-diisopropylethylamine (0.006 mL, 0.03411 mmol) were added. The reaction ran for

48 hours at room temperature (23°C) and mixed by sonication. Roto-vaped to dryness and crashed out product with Diethyl Ether. Solids were filtered out to produce corresponding product(0.0876 g, 0.01296 mmol, 95%)

13.8.5 Tetra-galactose modified polymer. To a solution of bis-galactose modified lysine linker (0.1726 g, 0.1364 mmol) in DCM, hydrogen chloride, 4M in 1,4-dioxane (682 μL,) was added and the reaction was run overnight at room temperature (23°C). The reaction was concentrated giving product bis-galactose lysine linker and used crude without any further purification. The next step was to make a solution of previous product of bis-galactose lysine linker (crude, 0.01364 mmol) and di-chlorotriazine PS-PEG (6.6 kD) (0.08766 g, 0.01296 mmol) in DCM. To this solution, N,N-diisopropylethylamine (0.0010 mL, 0.05456 mmol) was added to the solution. This reaction was run at 70°C for 1 hour in the Microwave to produce product.

13.8.6 Modified fucose benzyl-benzoate. To a solution of fucose-Br(OAc)$_3$ (2.007 g, 5.684 mmol) in DCM (34.1 mL, 1.5M) at 0°C, was added benzyl-4-hydroxylbenzoate (2.659 g, 11.652 mmol) and tetrabutylammonium hydrogensulfate (1.968 g, 5.798 mmol) stirring. 1M NaOH (11.4 mL, 0.5M) was added to form the biphasic mixture. After 72hrs the solution, now at room tempurature, was diluted with 30 mL of DCM, washed with water, brine, dried with sodium sulfate, and concentrated to dryness. A caramel consistant residue was purified using hexanes and ethyl acetate in a 100g column, where product elution occurred at 38% and elution of excess unreacted benzyl-4-hydroxylbenzoate eluted at 36-37%. Repurification was preformed at 10 column volumes over a generous gradient at 35-40%, elututing product in 20.6% yeild.

13.8.7 Modified fucose benzoate-acid. Fucose benzyl-benzoate (0.5717 g, 1.1746 mmol) was dissolved in THF (5.7mL, 0.1 M) and palladium on hydroxide (12%, 68 mg) was added to the reaction flask at room temperature. Hydrogen was added via balloon and the reaction was stirred overnight at room temperature. The residue was separated by vacuum filtration with a thin layer of celite washing with THF to yield 76%.

13.8.8 Bis-fucose-triacetate-boc-benzylamine-lysine. To a solution of bis-fmoc lysine mono-boc linker (0.160 g, 0.4746 mmol) in THF, 1,8-Diazabicyclo[5.4.0]undec-7-ene (0.301 mL, 1.978 mmol) was added. This reaction was stirred at room temperature for 30 minutes. The reaction was treated with 10 mL of diethyl ether and stirred for 5 minutes then placed into the freezer for 30 minutes. The supernatant was removed and the solids were concentrated and used crude (lysine mono-boc linker) without further purification. The crude product (0.1978 mmol) was made into a solution with DMF and modified L-fucose (0.1948 g, 0.4746 mmol) at room temperature. To this solution, N,N-diisopropylethylamine (0.072 mL, 0.989 mmol) and (Benzotriazol-1-yloxy) tripyrrolidinophosphonium hexafluorophosphate (0.3216 g, 0.6180 mmol) were added and stirred for 4 hours at room temperature (23°C). Once done, the reaction was quenched with water (50 mL) and vacuum filtered. The white solids were extracted and concentrated to yield product 10 (0.292 g, 0.231 mmol, 93.4%)

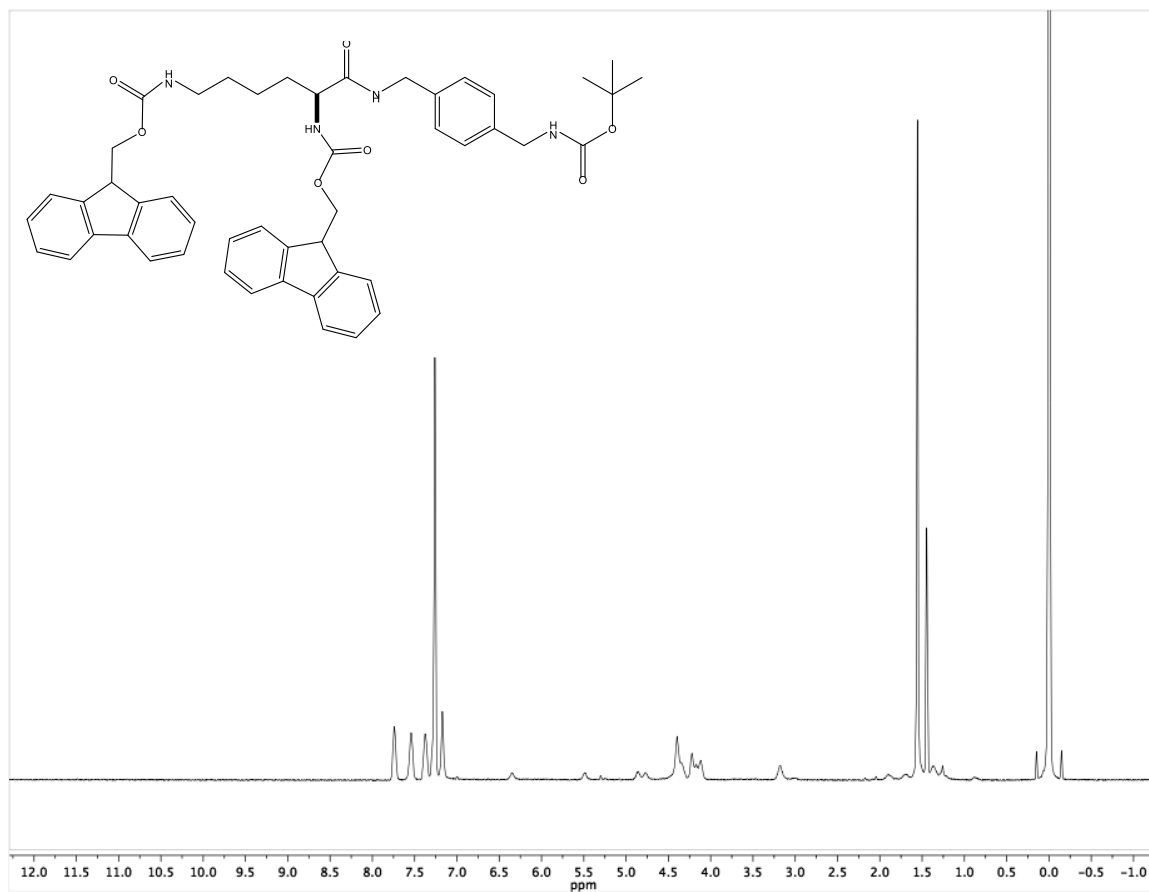**13.9 H-NMR and C-NMR of Intermediates and Product**

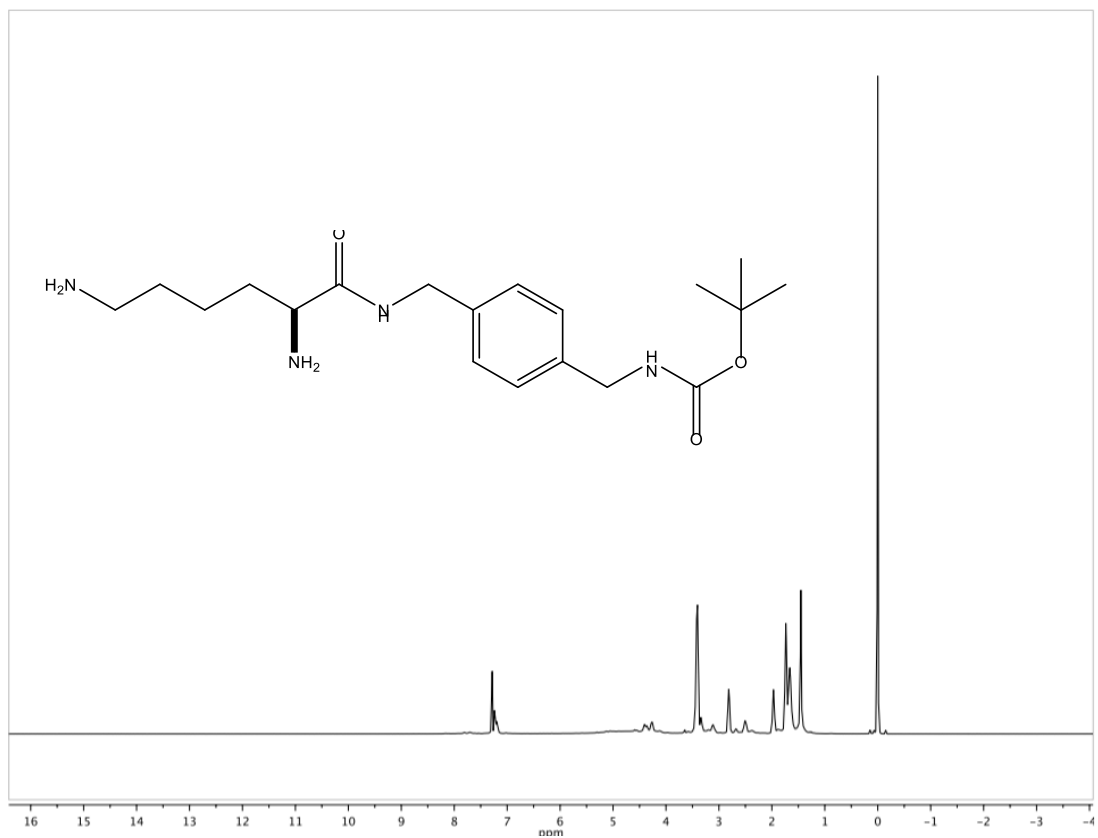*Figure 17*. H-NMR of bis-fmoc-boc-benzyldiamine-lysine

Figure 18. H-NMR of intermediate fmoc deprotection of bis-fmoc-benzyldiamine-lysine-boc
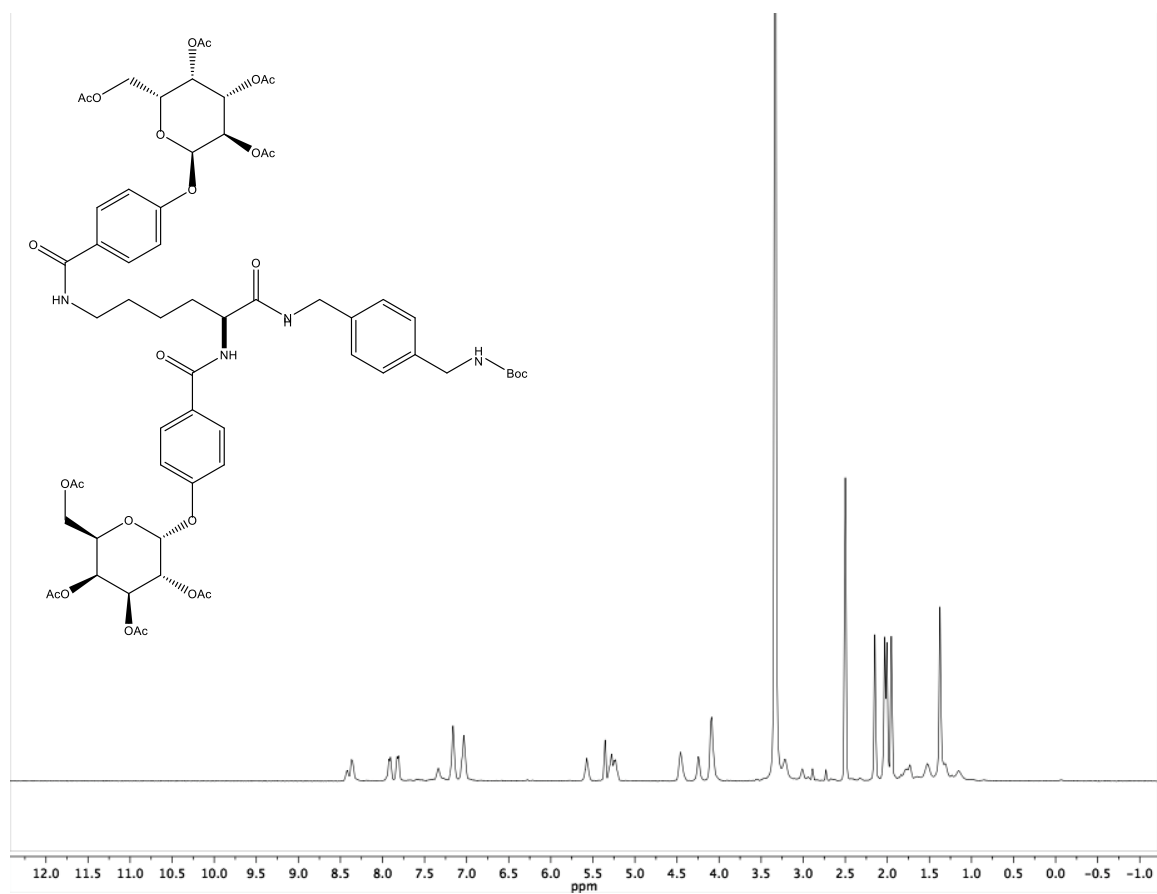
Figure 19. H-NMR of bis-benzoate-galactose(OAc)4-boc-benzyldiamine-lysine

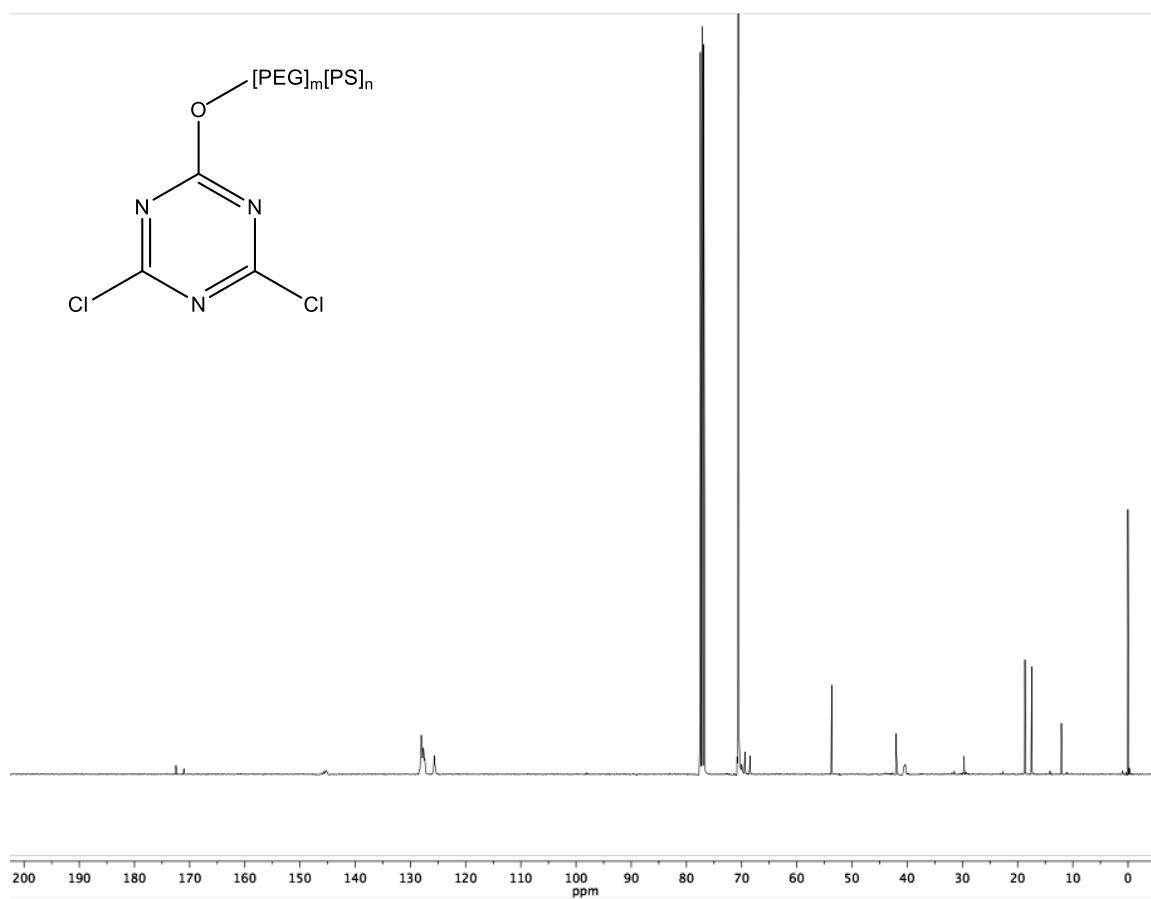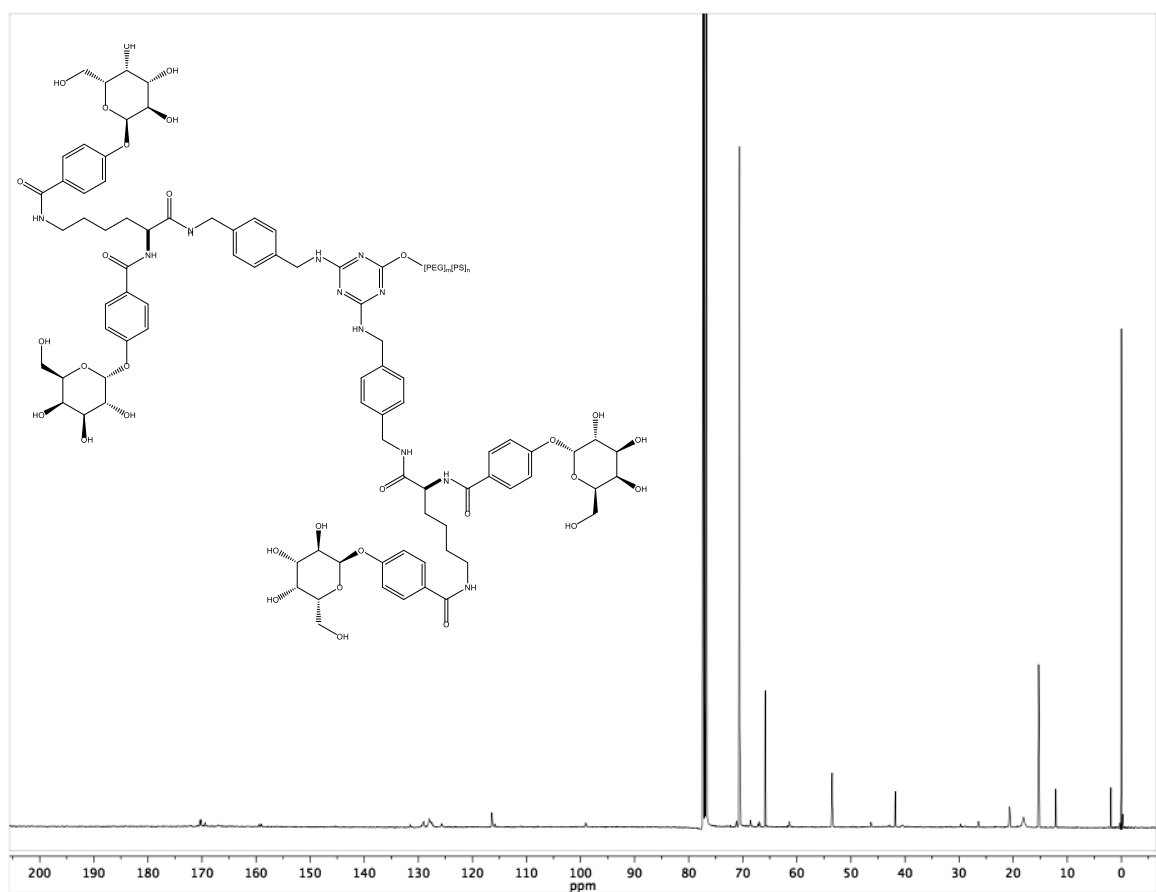*Figure 20.* C-NMR of PS-PEG modified cyanic chloride

Figure 21. H-NMR of tetra-benzoate-tetraactetate-galactose-bis-benzyldiamine-lysine on PS-PEG modified cyanuric chloride
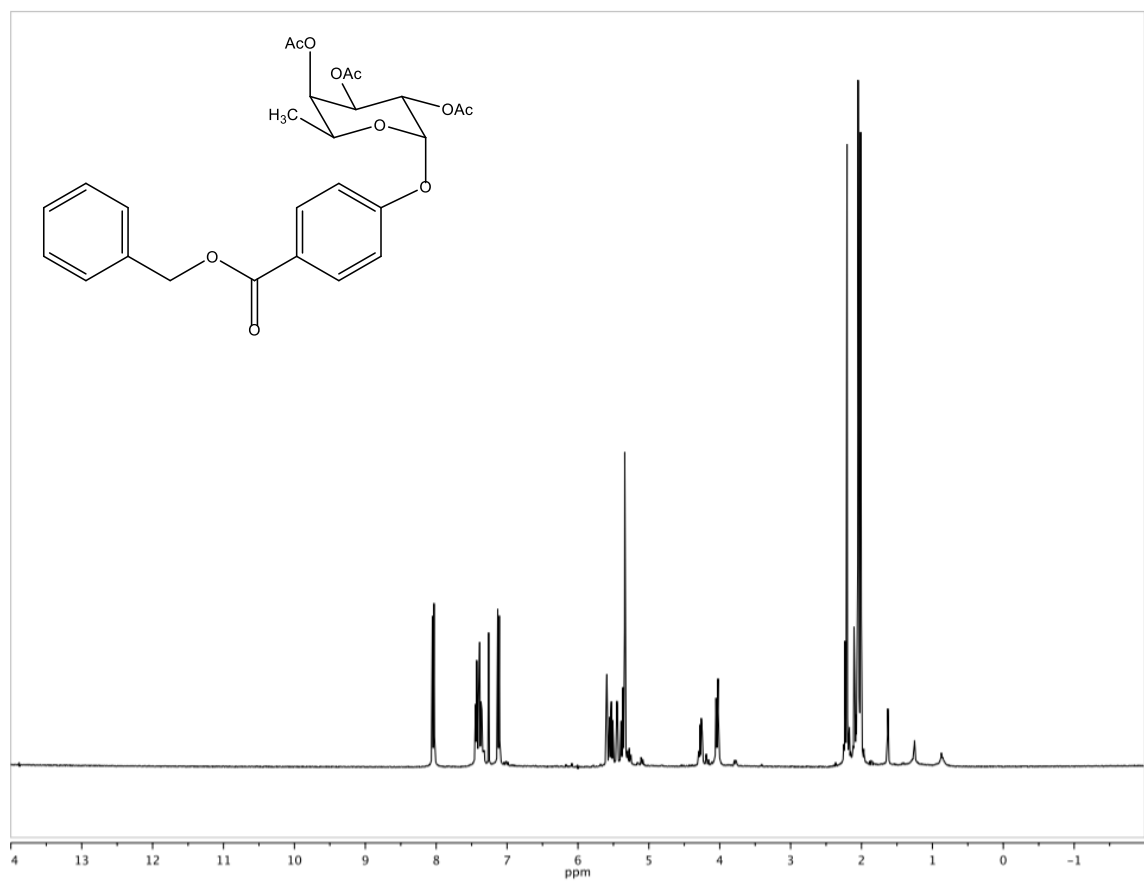
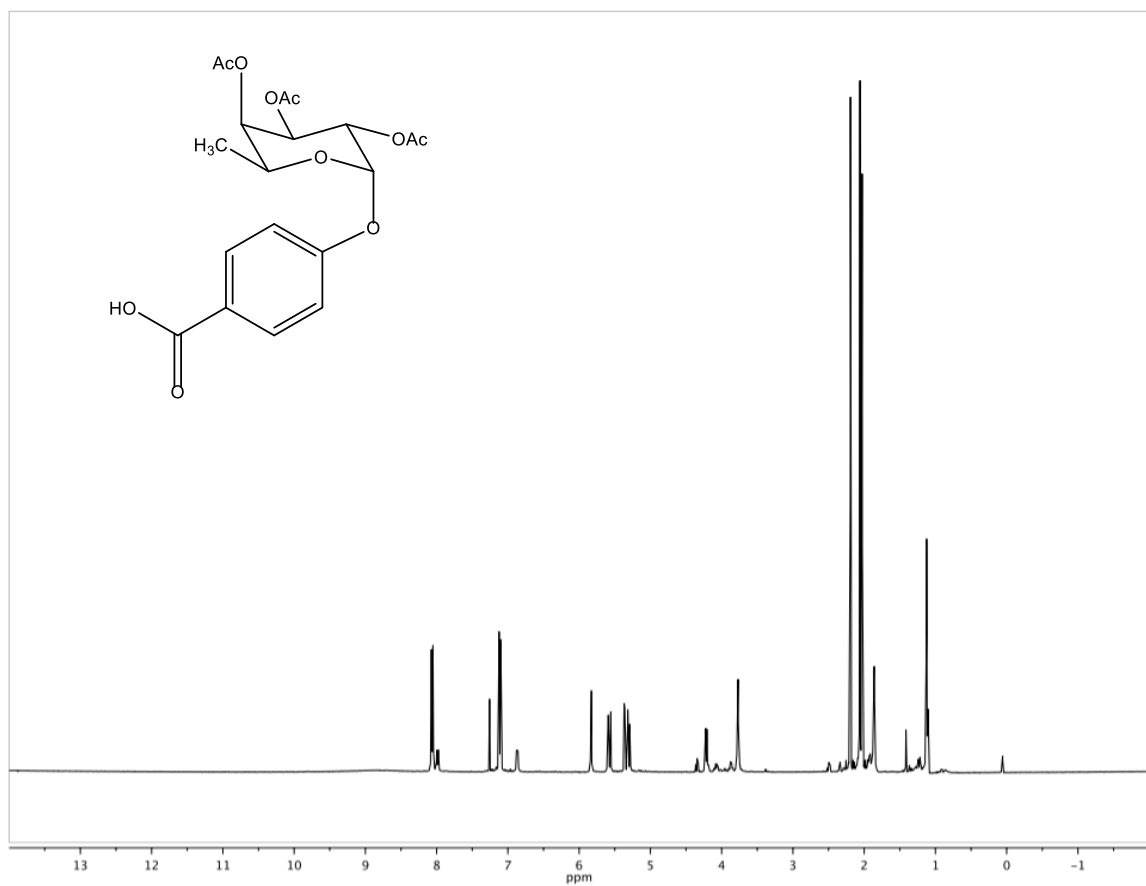*Figure 22.* H-NMR of modified fucose benzyl-benzoate

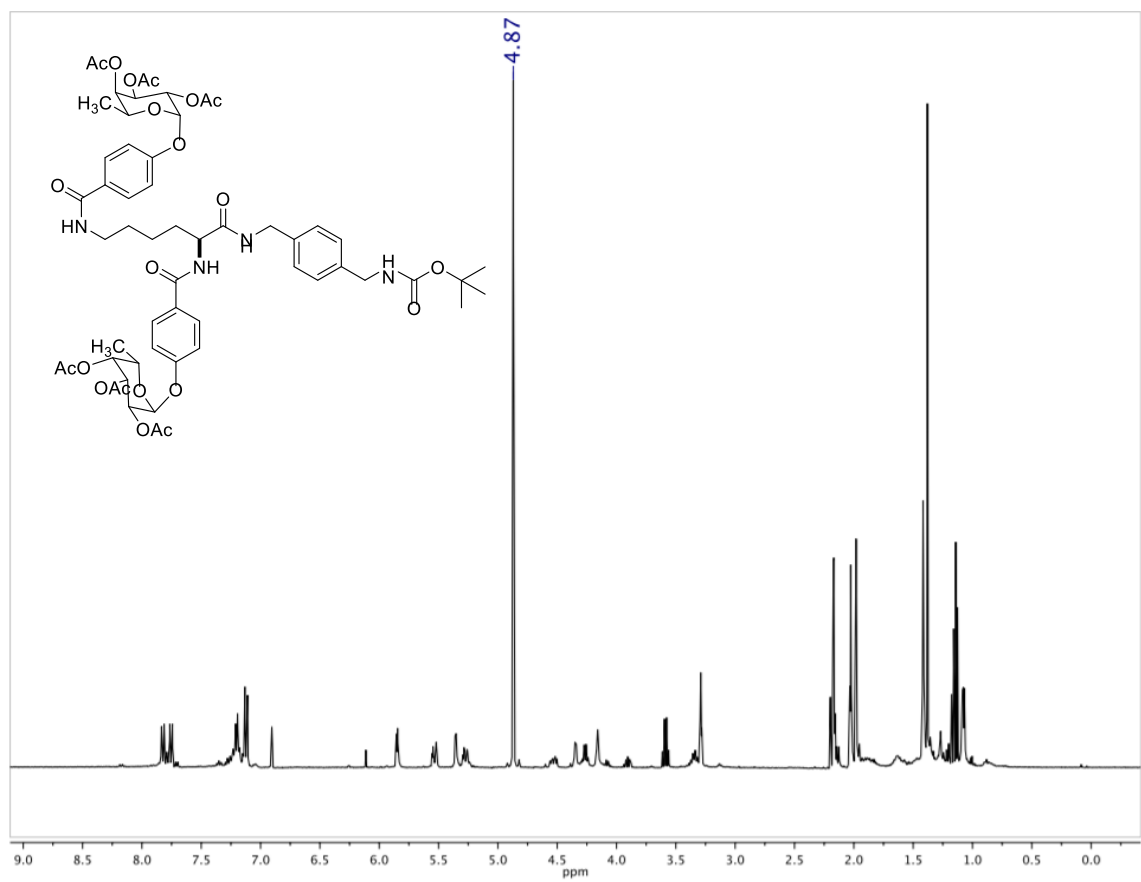*Figure 23.* H-NMR of fucose benzoate-acid

Figure 24. H-NMR bis-fucose-triacetate-boc-benzylamine-lysine
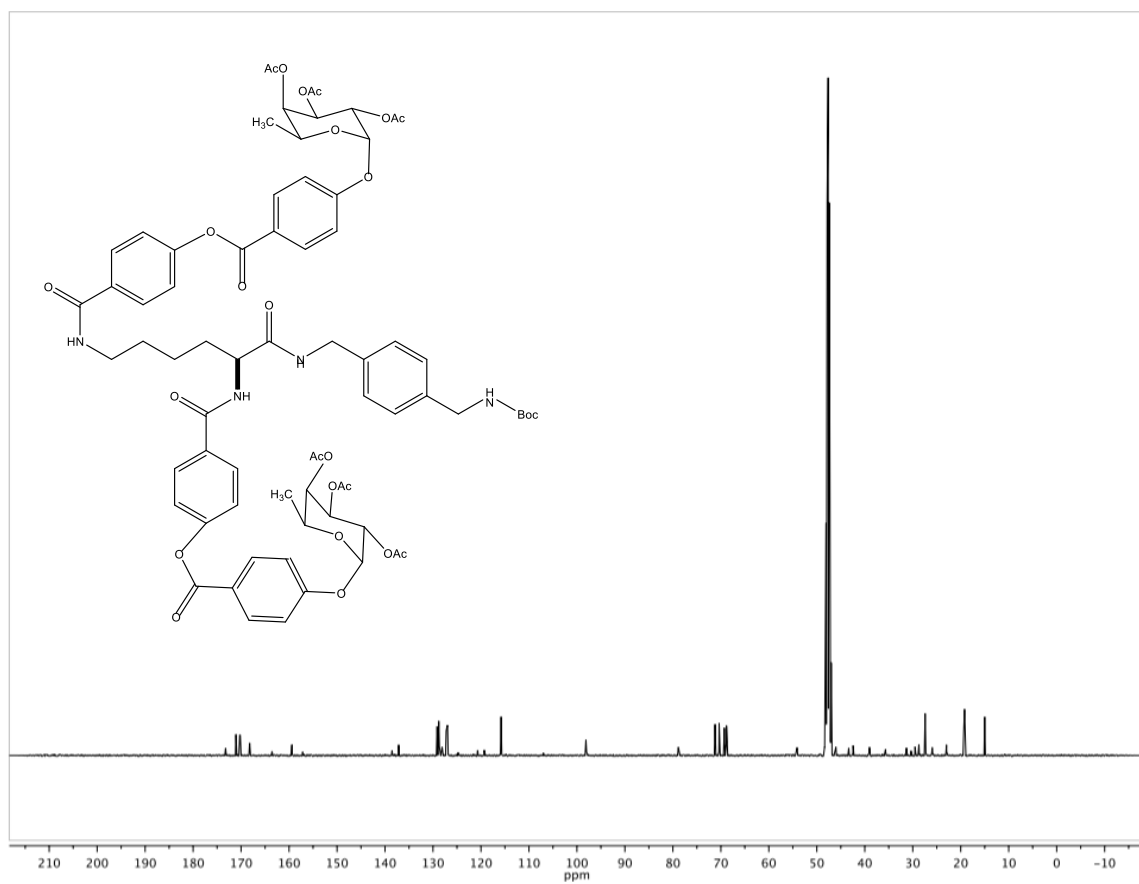
Figure 25. C-NMR of bis-fucose-triacetate-boc-benzylamine-lysine

References

1. Fischbach, M.A.; Walsh, C.T. Antibiotics for emerging pathogens. *Science* **2009**, 325, 1089–1093.

2. Hirsch, E.B.; Tam, V.H. Impact of multidrug-resistant Pseudomonas aeruginosainfection on patient outcomes. *Expert Rev. Pharmacoeconom. Outcomes Res.* **2010**, *10*, 441–451.

3. Brown, E.D.; Wright, G.D. Antibacterial drug discovery in the resistance era. *Nature* **2016**, *529*, 336–343.

4. Sun, H.-Y. Pneumonia Due to Pseudomonas aeruginosa. *Chest* **2011**, *139*, 1172.

5. Wright, G.D. The antibiotic resistome: The nexus of chemical and genetic diversity. *Nat. Rev. Microbiol.* **2007**, *5*, 175–186.

6. Lister, P.D.; Wolter, D.J.; Hanson, N.D. Antibacterial-resistant *Pseudomonas aeruginosa*: Clinical impact and complex regulation of chromosomally encoded resistance mechanisms. *Clin. Microbiol. Rev.* **2009**, *22*, 582–610.

7. Centers for Disease Control and Prevention. *Antibiotic Resistance Threats in the United States*; US Department of Health and Human Services: Washington, DC, USA, 2013. Available online: https://www.cdc.gov/drugresistance/biggest_threats.html (accessed on 4 September 2019).

8. Oliver, A. High frequency of hypermutable *Pseudomonas aeruginosa* in cystic fibrosis lung infection. *Science* **2000**, *288*, 1251–1253.

9. Deretic, V.; Schurr, M.J.; Boucher, J.C.; Martin, D.W. Conversion of *Pseudomonas aeruginosa* to mucoidy in cystic fibrosis: Environmental stress and regulation of bacterial virulence by alternative sigma factors. *J. Bacteriol.* **1994**, *176*, 2773–2780.

10. Wagner, S.; Sommer, R.; Hinsberger, S.; Lu, C.; Hartmann, R.W.; Empting, M.; Titz, A. Novel strategies for the treatment of *Pseudomonas aeruginosa* infections. *J. Med. Chem.* **2016**, *59*, 5929–5969.

11. Hadinoto, K.; Cheow, W.S. Nano-antibiotics in chronic lung infection therapy against Pseudomonas aeruginosa. *Colloids Surf. B Biointerf.* **2014**, *116*, 772–785.

12. Grishin, A.V.; Krivozubov, M.S.; Karyagina, A.S.; Gintsburg, A.L. Pseudomonas *Aeruginosa Lectins* as targets for novel antibacterials. *Acta Nat.* **2015**, *7*, 29–41.

13. Winzer, K.; Falconer, C.; Garber, N.C.; Diggle, S.P. The *Pseudomonas aeruginosa* lectins PA-IL and PA-IIL are controlled by quorum sensing and by RpoS. *J. Bacteriol.* **2000**, *182*, 6401–6411.

14. Mattmann, M.E.; Blackwell, H.E. Small molecules that modulate quorum sensing and control virulence in *Pseudomonas aeruginosa*. *J. Org. Chem.* **2010**, *75*, 6737–6746.

15. Tielker, D.; Hacker, S.; Loris, R.; Strathmann, M.; Wingender, J.; Wilhelm, S.; Rosenau, F.; Jaeger, K.-E. *Pseudomonas aeruginosa* lectin LecB is located in the outer membrane and is involved in biofilm formation. *Microbiology* **2005**, *151*, 1313–1323.

16. Imberty, A.; Wimmerova, M.; Mitchell, E.P. Structures of the lectins from Pseudomonas aeruginosa: Insights into the molecular basis for host glycan recognition. *Microbes Infect.* **2004**, *6*, 221–228.

17. Chemani, C.; Imberty, A.; de Bentzmann, S.; Pierre, M.; Wimmerova, M.; Guery, B.P.; Faure, K. Role of lecA and lecB lectins in *Pseudomonas aeruginosa*-induced lung injury and effect of carbohydrate ligands. *Infect. Immun.* **2009**, *77*, 2065–2075.

18. Lu, H.D.; Yang, S.S.; Wilson, B.K.; McManus, S.A.; Chen, C.V.H.H.; Prud'homme, R.K. Nanoparticle targeting of gram-positive and gram-negative bacteria for magnetic-based separations of bacterial pathogens. *Appl. Nanosci.* **2017**, *7*, 83–93.

19. D'addio, S.M.; Prud'homme, R.K. Controlling drug nanoparticle formation by rapid precipitation. *Adv. Drug Deliv. Rev.* **2011**, *63*, 417–426.

20. Cecioni, S.; Imberty, A.; Vidal, S. Glycomimetics versus multivalent glycoconjugates for the design of high affinity lectin ligands. *Chem. Rev.* **2015**, *115*, 525–561.

21. Peeters, E.; Nelis, H.J.; Coenye, T. Comparison of multiple methods for quantification of microbial biofilms grown in microtiter plates. *J. Microbiol. Methods* **2008**, *72*, 157–165.

22. Coenye, T.; Nelis, H.J. In vitro and in vivo model systems to study microbial biofilm formation. *J. Microbiol. Methods* **2010**, *83*, 89–105.

23. Drescher, K.; Shen, Y.; Bassler, B.L. Biofilm streamers cause catastrophic disruption of flow with consequences for environmental and medical systems. *Proc. Nat. Acad. Sci. USA* **2013**, *110*, 4345–4350.

24. O'Brien, K.T.; Noto, J.G.; Nichols-O'Neill, L.; Perez, L.J. Potent irreversible inhibitors of LasR quorum sensing in *Pseudomonas aeruginosa*. *ACS Med. Chem. Lett.* **2015**, *6*, 162–167.

25. Rahme, L.G.; Stevens, E.J.; Wolfort, S.F.; Shao, J.; Tompkins, R.G.; Ausubel, F.M. Common virulence factors for bacterial pathogenicity in plants and animals. *Science* **1995**, *268*, 1899–1902.

26. Capilato, J.N.; Philippi, S.V.; Reardon, T.; McConnell, A.; Oliver, D.C.; Warren, A.; Adams, J.; Wu, C.; Perez, L.J. Development of a novel series of non-natural triaryl

agonists and antagonists of the Pseudomonas aeruginosa LasR quorum sensing receptor. *Bioorg. Med. Chem.* **2017**, *25*, 153–165.

27. Titz, A. Carbohydrate-based anti-virulence compounds against chronic *Pseudomonas aeruginosa* Infections with a focus on small molecules. *Top. Med. Chem.* **2014**, *12*, 169–186.

28. Imberty, A.; Chabre, Y.M.; Roy, R. Glycomimetics and glycodendrimers as high affinity microbial anti-adhesins. *Chem. Eur. J.* **2008**, *14*, 7490–7499.

29. Bajolet-Laudinat, O.; Girod-de Bentzmann, S.; Tournier, J.M.; Madoulet, C.; Plotkowski, M.C.; Chippaux, C.; Puchelle, E. Cytotoxicity of *Pseudomonas aeruginosa* internal lectin PA-I to respiratory epithelial cells in primary culture. *Infect. Immun.* **1994**, *62*, 4481–4487.

30. Carlmark, A.; Hawker, C.; Hult, A.; Malkoch, M. New methodologies in the construction of dendritic materials. *Chem. Soc. Rev.* **2009**, *38*, 352–362.

31. Grayson, S.M.; Frechet, J. Convergent dendrons and dendrimers: From synthesis to applications. *Chem. Rev.* **2001**, *101*, 3819–3868.

32. Singh, R.; Lillard, J.W. Nanoparticle-based targeted drug delivery. *Exp. Mol. Pathol.* **2009**, *86*, 215–223.

33. Bogart, L.K.; Pourroy, G.; Murphy, C.J.; Puntes, V.; Pellegrino, T.; Rosenblum, D.; Peer, D.; Lévy, R. Nanoparticles for imaging, sensing, and therapeutic intervention. *ACS Nano* **2014**, *8*, 3107–3122.

34. Zhu, X.; Radovic-Moreno, A.F.; Wu, J.; Langer, R.; Shi, J. Nanomedicine in the management of microbial infection—Overview and perspectives. *Nano Today* **2014**, *9*, 478–498.

35. Huh, A.J.; Kwon, Y.J. "Nanoantibiotics": A new paradigm for treating infectious diseases using nanomaterials in the antibiotics resistant era. *J. Control. Release* **2011**, *156*, 128–145.

36. Kalhapure, R.S.; Suleman, N.; Mocktar, C.; Seedat, N.; Govender, T. Nanoengineered drug delivery systems for enhancing antibiotic therapy. *J. Pharm. Sci.* **2015**, *104*, 872–905.

37. Pelgrift, R.Y.; Friedman, A.J. Nanotechnology as a therapeutic tool to combat microbial resistance. *Adv. Drug Deliv. Rev.* **2013**, *65*, 1803–1815.

38. Lu, H.D.; Spiegel, A.C.; Hurley, A.; Perez, L.J.; Maisel, K.; Ensign, L.M.; Hanes, J.; Bassler, B.L.; Semmelhack, M.F.; Prud'homme, R.K. Modulating Vibrio cholerae

quorum-sensing-controlled communication using autoinducer-loaded nanoparticles. *Nano Lett.* **2015**, *15*, 2235–2241.

39. D'Addio, S.M.; Baldassano, S.; Shi, L.; Cheung, L.; Adamson, D.H.; Bruzek, M.; Anthony, J.E.; Laskin, D.L.; Sinko, P.J.; Prud'homme, R.K. Optimization of cell receptor-specific targeting through multivalent surface decoration of polymeric nanocarriers. *J. Control. Release* **2013**, *168*, 41–49.

40. O'Toole, G.A. Microtiter dish biofilm formation assay. *J. Vis. Exp.* **2011**, *47*, 2437.

41. Han, J.; Zhu, Z.; Qian, H.; Wohl, A.R.; Beaman, C.J.; Hoye, T.R.; Macosko, C.W. A Simple Confined Impingement Jets Mixer for Flash Nanoprecipitation. *J. Pharm. Sci.* **2012**, *101,* 4018–4023.

42. Müsken, M.; Di Fiore, S.; Römling, U.; Häussler, S. A 96-well-plate–based optical method for the quantitative and qualitative evaluation of Pseudomonas aeruginosa biofilm formation and its application to susceptibility testing. *Nat. Protoc.* **2010**, *5*, 1460–1469.

43. Heydorn, A.; Nielsen, A.T.; Hentzer, M.; Sternberg, C.; Givskov, M.; Ersbøll, B.K.; Molin, S. Quantification of biofilm structures by the novel computer program COMSTAT. *Microbiology* **2000**, *146*, 2395–2407.

44. Vorregaard, M. Comstat2—A Modern 3D Image Analysis Environment for Biofilms, in Informatics and Mathematical Modelling. Master's Thesis, Technical University of Denmark, Kongens Lyngby, Denmark, 31 January **2008**. Available online: www.comstat.dk (accessed on 4/23/2019).

45. Huthmacher, K.; Most, D. Cyanuric Acid and Cyanuric Chloride. *Ullmanns Encyclopedia of Industrial Chemistry* **2000**.

46. Sommer, R.; Rox, K.; Wagner, S.; Hauck, D.; Henrikus, S. S.; Newsad, S.; Arnold, T.; Ryckmans, T.; Brönstrup, M.; Imberty, A.; Varrot, A.; Hartmann, R. W.; Titz, A. Anti-Biofilm Agents against Pseudomonas Aeruginosa: A Structure–Activity Relationship Study of C-Glycosidic LecB Inhibitors. *Journal of Medicinal Chemistry* **2019**, *62* (20), 9201–9216..